Biochemical and Biophysical Research Communications 371 (2008) 104–109

Contents lists available at ScienceDirect

Biochemical and Biophysical Research Communications

journal homepage: www.elsevier.com/locate/ybbrc

New efficient replication system with hepatitis C virus genome derived from a patient with acute hepatitis C ☆

Kyoko Mori, Ken-ichi Abe, Hiromichi Dansako, Yasuo Ariumi, Masanori Ikeda, Nobuyuki Kato *

Department of Molecular Biology, Okayama University Graduate School of Medicine, Dentistry, and Pharmaceutical Sciences, 2-5-1 Shikata-cho, Okayama 700-8558, Japan

ARTICLE INFO

Article history:
Received 25 March 2008
Available online 10 April 2008

Keywords:
Hepatitis C virus
Acute hepatitis C
HCV replication system
Genome-length HCV RNA
Anti-HCV reagents
Interferon-γ

ABSTRACT

We report for the first time a new RNA replication system with a hepatitis C virus (HCV) strain (AH1) derived from a patient with acute hepatitis C. Using an HCV replicon RNA library constructed with the AH1 strain (genotype 1b), we first established a cloned cell line, sAH1, harboring the HCV replicon. Cured cells obtained with interferon treatment of sAH1 cells were used for transfection with genome-length HCV RNA possessing four mutations found in sAH1 replicon. Consequently, one cloned cell line, AH1, supporting efficient replication of genome-length HCV RNA was obtained. By the comparison of AH1 cells with the O cells supporting genome-length HCV RNA (HCV-O strain) replication, we found different anti-HCV profiles of interferon-γ and cyclosporine A between AH1 and O cells. Reporter assay analysis suggests that the diverse effects of interferon-γ are due to the difference in HCV strains, but not the cellular environment.

© 2008 Elsevier Inc. All rights reserved.

Hepatitis C virus (HCV) infection frequently causes chronic hepatitis, which progresses to liver cirrhosis and hepatocellular carcinoma. HCV infection has now become a serious health problem because at least 170 million people worldwide are currently infected with HCV [1]. HCV is an enveloped virus with a positive single-stranded 9.6 kilobase (kb) RNA genome, which encodes a large polyprotein precursor of approximately 3000 amino acid (aa) residues [2,3]. This polyprotein is cleaved by a combination of the host and viral proteases into at least 10 proteins in the following order: core, envelope 1 (E1), E2, p7, non-structural 2 (NS2), NS3, NS4A, NS4B, NS5A, and NS5B [3].

As a striking breakthrough in HCV research, in 1999, an HCV replicon system enabling robust HCV subgenomic RNA (Con-1 strain of genotype 1b) replication in specific human HuH-7 hepatoma cells has been developed [4]. After the first Con-1 replicon, several HCV replicon (genotypes 1a, 1b, and 2a) systems using HuH-7-derived cells have been developed. These replicon systems have become powerful tools for basic studies of HCV replication, HCV–host cell interactions, and screening of anti-HCV reagents, [5,6]. Furthermore, genome-length HCV RNA replication systems have been developed [7–9], since HCV replicons lacking HCV structural proteins are insufficient for further HCV research. We also established a genome-length HCV RNA-replicating cell line (HCV-O strain of genotype 1b; called O cell line) [10] using cured cells derived from sO cells [11], in which HCV replicon RNA (HCV-O strain) with an adaptive mutation (S2200R) is replicating. However, to date, established genome-length HCV RNA-replicating stable cell lines are limited to five HCV strains, H77 (1a), HCV-N (1b), Con-1 (1b), HCV-O (1b), and JFH1 (2a) [7–10,12], and there is no RNA replication system with an HCV strain derived from a patient with acute hepatitis C. Furthermore, there have been few reports comparing these HCV strains.

To clarify these problems, we have attempted to establish a new stable cell line, in which genome-length HCV RNA derived from a patient with acute hepatitis C is efficiently replicating. We report herein a new efficient RNA replication system with HCV derived from a patient with acute hepatitis C and provide a comparative analysis of RNA replication systems with AH1 and HCV-O strains regarding the sensitivities to anti-HCV reagents, including interferon (IFN)-α.

Materials and methods

Cell culture. Cells supporting HCV replicon or genome-length HCV RNA, and cured cells, from which the HCV RNA had been eliminated by IFN treatment, were maintained as described previously [10].

Reverse transcription (RT)-nested PCR. RNA from a serum of patient AH1 [13] with acute hepatitis C was prepared using the ISOGEN-LS extraction kit (Nippon Gene Co., Japan). This RNA sample was used as a template for RT-nested PCR to amplify the HCV RNA. RT-nested PCR was performed separately in two parts; one part (3.5 kb) covered from HCV 5′UTR to NS3, and the other part (6 kb) covered from NS2 to NS5B. For the first part, the antisense primer AH3553R, 5′-CACACGCCGTTGATGC AGGTCG-3′ was used for RT. Primers 21 [11] and AH3519R, 5′-TGCGTGGCGG

☆ The nucleotide sequence data reported in this paper will appear in the DDBJ, EMBL, and GenBank nucleotide sequence databases under Accession No. AB429050.

* Corresponding author. Fax: +81 86 235 7392.
E-mail address: nkato@md.okayama-u.ac.jp (N. Kato).

0006-291X/$ - see front matter © 2008 Elsevier Inc. All rights reserved.
doi:10.1016/j.bbrc.2008.04.005

TGGAAACCACCTG-3′ were employed in the first round of PCR (35 cycles). An internal primer pair (21X [11] and AH3466RX: 5′-ATTATTCTAGAGGCCTGTGAGACTG GTGATGATGC-3′; containing a XbaI site (underlined)) was used for the second round of PCR (35 cycles). For the second part, the antisense primer 386R [11] was used for RT. Primers 542 and 9388R [11] were employed in the first round of PCR (35 cycles). An internal primer pair (3295X: 5′-ATTATTCTAGACTGACATGGA GACCAAGATCATCAC-3′; containing a XbaI site (underlined) and 9357RX: 5′-ATTATT CTAGACCCGTTCACCGGTTGGGGAGCAG-3′; containing a XbaI site (underlined)) was used for the second round of PCR (35 cycles). These fragments overlapped at the NS2 and NS3 regions and were used for sequence analysis for HCV RNA after cloning into the XbaI site of pBR322MC [11]. Superscript II (Invitrogen) and KOD-plus DNA polymerase (Toyobo, Osaka, Japan) were used for RT and PCR, respectively.

Plasmid construction. PCR product (NS3 to NS5B of AH1 strain) with primers 542 and 9388R was further amplified with primers 3501S: 5′-ATTATACTAGTCTCACAGG CCGGGACAAGAACC-3′; containing a SpeI site (underlined) and 9162RB: 5′-ATTATC GTACGGCCCAGTTGAAGAGGTACTTGCC-3′; containing a BsiWI site (underlined). The amplified fragment was digested with SpeI and BsiWI, and ligated into the replicon cassette plasmid pNSS1RZ2RU [11], which was predigested with SpeI and BsiWI. Using this ligation reaction mixture, a replicon RNA library (AH1N/3-5B in Supplementary Fig. 1) was prepared by a previously described method [11]. To make the plasmid pAH1N/C-5B/PL, LS, $(VA)_2$ containing full-length HCV polyprotein of AH1 strain, pON/C-5B containing full-length HCV polyprotein of HCV-O strain [10] was utilized. First, to make a fragment for pAH1N/C-5B (Supplementary Fig. 1), overlapping PCR was used to fuse EMCV IRES to the core protein-coding sequence of the AH1 strain, as described previously [10]. The resulting DNA was digested with PmeI and ClaI, and then replaced with the PmeI–ClaI fragment of pON/C-5B (pON/C-5B/CoreAH was obtained). Second, the ClaI–AgeI fragment of pHCV-AH1 containing full-length HCV polyprotein of AH1 strain was replaced with the ClaI–AgeI fragment of pON/C-5B/CoreAH (pAH1N/C-5B was obtained). Finally, the SpeI–BsiWI fragment of pAH1N/3-5B clone 2 (see Fig. 1C) was replaced with the SpeI–BsiWI fragment of pAH1N/C-5B (pAH1N/C-5B/PL, LS, $(VA)_2$ was obtained).

RNA synthesis. Plasmid DNAs were linearized by XbaI and were used for RNA synthesis with T7 MEGAscript (Ambion) as previously described [11].

RNA transfection and selection of G418-resistant cells. The transfection of HCV replicon RNA or genome-length HCV RNA synthesized in vitro into HuH-7-derived cells was performed by electroporation, and the cells were selected in the presence of G418 (0.3 mg/ml; Promega) for 3 weeks as described previously [11].

Quantification of HCV RNA. The quantitative RT-PCR (RT-qPCR) analysis for HCV RNA was performed by LightCycler PCR as described previously [10]. Experiments were done in triplicate.

Integration analysis. Genomic DNA was extracted from the cultured cells using the DNeasy Blood & Tissue Kit (QIAGEN). The HCV 5′UTR and the IFN-β gene were detected according to a PCR method described previously [11].

Western blot analysis. The preparation of cell lysates, sodium dodecyl sulfate–polyacrylamide gel electrophoresis, and immunoblotting analysis were performed as previously described [11]. The antibodies used in this study were those against Core, E2, NS3, NS4A, NS5A, and NS5B [10]. β-Actin antibody (AC-15, Sigma) was used as the control for the amount of protein loaded per lane. Immunocomplexes were detected with the Renaissance enhanced chemiluminescence assay (Perkin-Elmer Life Sciences, Boston, MA).

Sequence analysis of HCV RNA. To amplify replicon RNA and genome-length HCV RNA, RT-PCR was performed as described previously [10,11]. The PCR products were subcloned into the XbaI site of pBR322MC, and sequence analysis was performed as described previously [11].

Northern blot analysis. Total RNA was extracted from the cultured cells using the RNeasy Mini Kit (QIAGEN). Three micrograms of total RNA was used for the analysis. HCV-specific RNA and β-actin were detected according to a method described previously [10].

Luciferase reporter assay. For the dual-luciferase assay, firefly luciferase vectors, pGBP-1(-216)-Luc and p2′–5′-OAS(-159)-Luc [14], were used. The reporter assay was performed as previously described [14]. The experiments were performed in at least triplicate.

Statistical analysis. Differences between AH1 and O cell lines were tested using the Student's *t*-test. *P* values <.05 were considered statistically significant.

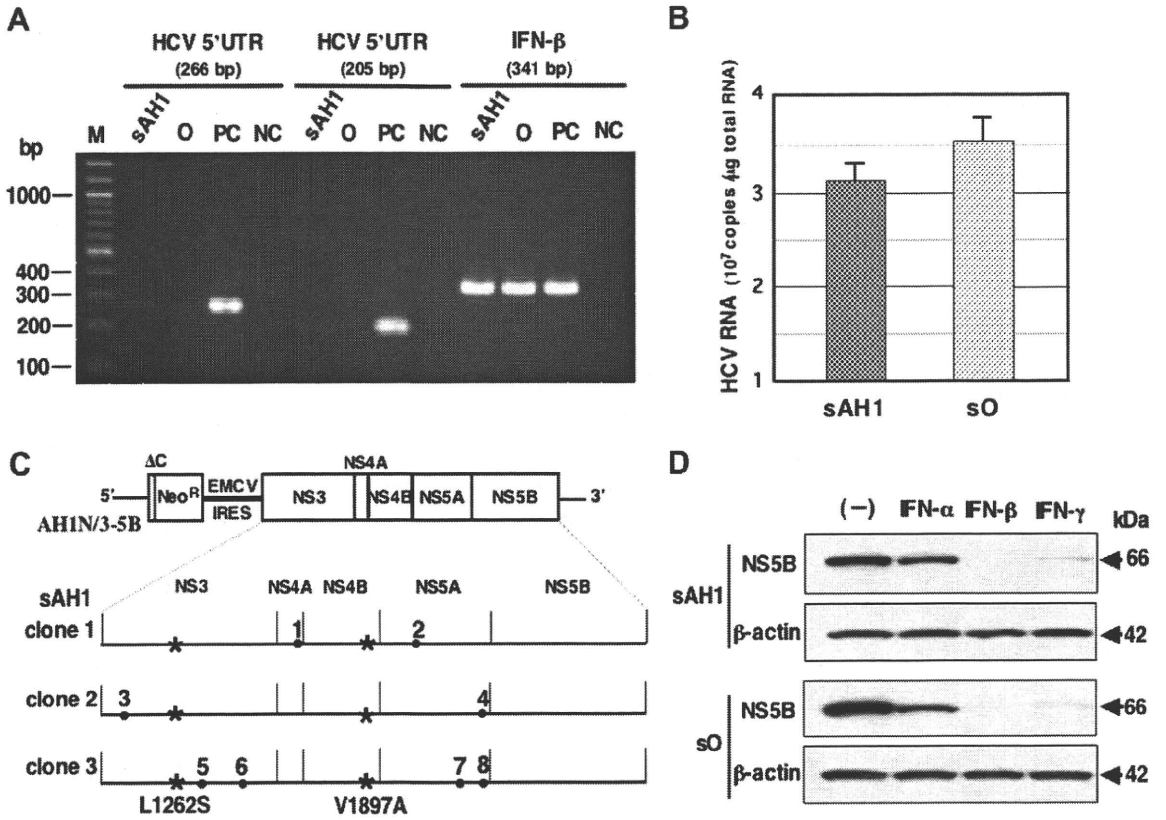

Fig. 1. Characterization of sAH1 cells harboring HCV replicon. (A) No integration of the HCV sequence in the genomic DNA. Genomic DNA from sAH1cells was subjected to PCR for the detection of the HCV 5′UTR and the IFN-β gene. O cells were used as a negative control. Lane PC, HCV sequence-integrated cells; lane NC, no genomic DNA; lane M, 100 bp DNA ladder. PCR products were detected by staining with ethidium bromide after 3% agarose gel electrophoresis. (B) Quantitative analysis of intracellular replicon RNA. The levels of replicon RNA were quantified by LightCycler PCR. sO cells harboring HCV-O replicon [11] were used for the comparison. (C) Amino acid substitutions detected in intracellular AH1 replicon RNA. NS3 to NS5B regions of three independent clones sequenced were presented. L1262S and V1897A conserved substitutions are indicated by asterisks. Clone-specific aa substitutions (indicated by the numbers with dots) are as follows: 1, K1691R; 2, M2105I; 3, P1115L; 4, V2360A; 5, K1368R; 6, A1533T; 7, I2285V; 8, D2377H. (D) IFN sensitivity of AH1 replicon. sAH1 cells were treated with IFN-α (Sigma), IFN-β (a gift from Toray Industries), and IFN-γ (Sigma) (20 IU/ml each) for 5 days. For the comparison, sO cells were treated as well as sAH1 cells. NS5B was detected by Western blot analysis.

Results

Establishment of a G418-resistant cell line (sAH1) harboring HCV replicon RNA

An HCV replicon RNA library prepared from the AH1 strain was first transfected into sOc cells (cured sO cells) [11], and the G418-resistant cells were selected as described previously [11]. Although several G418-resistant colonies were obtained, production of these colonies was due to integration of the HCV RNA sequence into the chromosomal DNA (PC in Fig. 1A). Therefore, we further cleaned up the replicon RNA library with additional DNase treatment, and it was then transfected into OR6c cells (cured OR6 cells) [10]. Consequently, a G418-resistant colony was obtained and successfully proliferated; this colony was referred to as sAH1. To exclude the possibility of integration of a replicon RNA sequence into the genomic DNA, we examined the presence of the HCV 5′UTR sequence in the genomic DNA isolated from sAH1 cells by a PCR method described previously [11]. Genome-length HCV RNA-replicating O cells were also examined as a negative control. The results revealed that the HCV RNA sequence was not integrated into the genomic DNA in either sAH1 cells or O cells (Fig. 1A).

Regarding the level of replicon RNA in sAH1 cells, RT-qPCR analysis revealed that the titer of replicon RNA was approximately 3×10^7 copies/μg total RNA, and its level was equivalent to that in sO cells (Fig. 1B), suggesting that the efficiency of RNA replication in sAH1 cells is similar to that in sO cells.

To exclude the possibility that sAH1 cells were derived from a small number of OR6 cells remaining after IFN treatment, and to determine whether replicon RNA in sAH1 cells possesses cell culture-adaptive mutations [5], which enhance the efficiency of RNA replication, we performed genetic analysis of the intracellular AH1 replicon. The sequences of three independent clones were determined and compared with each other to avoid PCR error. The obtained consensus nucleotide and aa sequences of NS3–NS5B regions of the AH1 replicon showed 7.3% and 3.7% differences, respectively, from those of the HCV-O replicon [11], indicating that sAH1 cells were not contaminated by the OR6 cells. In contrast, to find conserved mutations in the AH1 replicon, we determined the consensus nucleotide sequences of AH1 serum-derived HCV RNA by comparison of the nucleotide sequences of three independently isolated cDNA clones (Accession No. AB429050). The K1609E (NS3) and S2200R (NS5A) adaptive mutations found in O and OR6 cells were not detected in the AH1 replicon. However, instead of these mutations, L1262S (NS3) and V1897A (NS4B) conserved mutations were detected (Fig. 1C). Although V1897A has been detected as an adaptive mutation in Con-1 replicon [15], L1262S has until now remained undetected. In clone 2, the P1115L mutation (number 3 in Fig. 1C), which has been reported as an adaptive mutation [15,16], was detected.

To further characterize the sAH1 replicon, we compared the sensitivities of sAH1 and sO replicons against anti-HCV reagents (IFN-α, IFN-β, and IFN-γ) [5,6,11]. Western blot analysis of NS5B revealed that the IFN sensitivity of the sAH1 replicon was equivalent to that of the sO replicon (Fig. 1D).

Establishment of a genome-length HCV-AH1 RNA-replicating cell line, AH1

To develop a genome-length HCV RNA replication system, we first constructed a pAH1N/C-5B/PL, LS, $(VA)_2$ by the replacement with sAH1 replicon clone 2 (Fig. 1C) into pAH1N/C-5B. AH1N/C-5B/PL, LS, $(VA)_2$ RNA was transfected into sAH1c cells, cured sAH1 cells. Following 3 weeks of culturing in the presence of

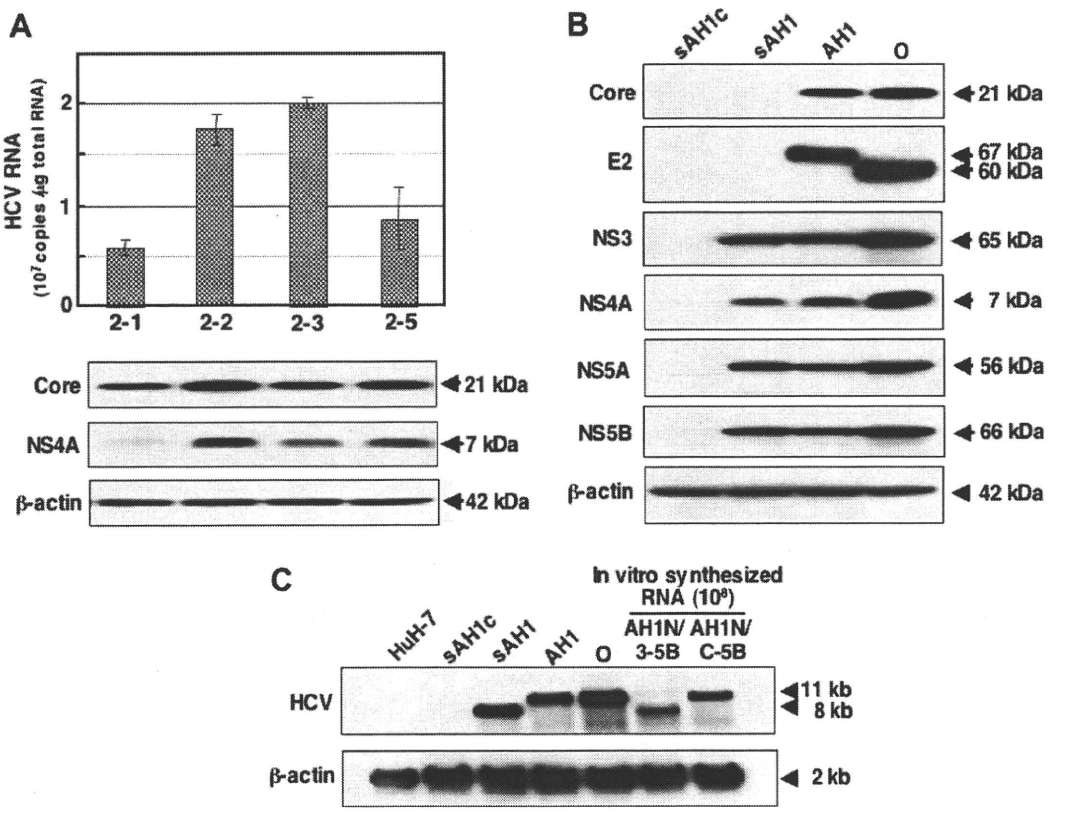

Fig. 2. Characterization of AH1 cells harboring genome-length HCV RNA. (A) Selection of G418-resistant cell lines. The levels of HCV RNA in G418-resistant cells were quantified by LightCycler PCR (upper panel). Core and NS4A were detected by Western blot analysis (lower panel). (B) Western blot analysis. AH1, O, sAH1, and sAH1c cells were used for the comparison. Core, E2, NS3, NS4A, NS5A, and NS5B were detected by Western blot analysis. (C) Northern blot analysis. AH1, O, sAH1, sAH1c, and HuH-7 cells were used for the comparison. In vitro-synthesized AH1N/3-5B and AH1N/C-5B RNAs were also used for the comparison.

G418, several colonies were obtained, and 4 colonies (2-1, 2-2, 2-3, and 2-5) then successfully proliferated. We selected colony 2-2 among them because it showed high levels of HCV RNA and proteins (core and NS4A) (Fig. 2A); this cell line was referred to as AH1. To compare the expression levels of HCV proteins in AH1 cells with those in O cells, Western blot analysis was further performed. Although the levels of HCV proteins in AH1 cells were slightly lower than those in O cells, the expression levels of NS proteins in AH1 cells were equivalent to those in sAH1 cells (Fig. 2B). In this analysis, we noticed that the size of the E2 protein in AH1 cells was 7 kDa larger than that in O cells (Fig. 2B). This difference may be due to the different numbers of *N*-glycosylation sites in E2 protein, since 11 and 9 *N*-glycosylation sites in E2 proteins are estimated in AH1 and HCV-O strains, respectively. Northern blot analysis also showed the presence of HCV-specific RNA with a length of approximately 11 kb in the extracts of total RNA prepared from AH1 cells, similar to that in the O cells (Fig. 2C). We confirmed the presence of replicon RNA (approximately 8 kb) in sAH1 cells (Fig. 2C). To check the additional adaptive mutations in the genome-length AH1 RNA, we performed sequence analysis of HCV RNA in AH1 cells. The results (Supplementary Fig. 2) revealed no additional mutations detected commonly among the three independent clones sequenced, suggesting that additional adaptive mutations are not required for genome-length HCV RNA replication. We therefore conclude that the AH1 cell line can be used as a genome-length HCV RNA replication system with acute hepatitis C-derived HCV strain.

Diverse effects of anti-HCV reagents on HCV RNA replication in AH1 and O cells

To compare the effects of anti-HCV reagents on RNA replication systems with different HCV strains, we examined the anti-HCV profiles of IFN-α, IFN-γ, and cyclosporine A (CsA) [17] using AH1 and O cells. Regarding IFN-α, the anti-HCV effect in AH1 cells was similar to that in O cells (Fig. 3A). Although RT-qPCR analysis showed a statistically significant difference in both cell systems when 1 IU/ml of IFN-α was used, such a difference was not observed in the Western blot analysis (Fig. 3A). In contrast, a significant different effect of IFN-γ was observed in both cell systems. RT-qPCR and Western blot analyses revealed that RNA replication of the AH1 strain was less sensitive than that of the HCV-O strain when 1 or 10 IU/ml of IFN-γ was used (Fig. 3B). Conversely, we observed that RNA replication of the AH1 strain was more sensitive to CsA than that of the HCV-O strain (Fig. 3C). These results suggest that anti-HCV profiles of IFN-γ and CsA are rather different between AH1 and O cell systems.

Different anti-HCV profile of IFN-γ is not correlated with the cellular potentials of the IFN-γ signaling pathway

To clarify whether the different effects of IFN-γ observed between AH1 and O cells are dependent on the cellular potentials of the IFN-γ signaling pathway, we performed a dual-luciferase reporter assay using an IFN-γ-inducible intrinsic GBP-1 gene promoter. As a control, IFN-α-inducible intrinsic 2′–5′-OAS gene promoter was also used for the analysis of the IFN-α signaling pathway. The results revealed that a good response of both AH1 and O cells to IFN-α and IFN-γ stimulation, with their potentials for both signaling pathways being almost the same (Fig. 4). These results suggest that the diverse anti-HCV effects of IFN-γ are dependent on the HCV strain, but not on the cellular potentials of the IFN-γ signaling pathway.

Discussion

In the present study, we established for the first time an HCV RNA replication system with AH1 strain derived from a patient

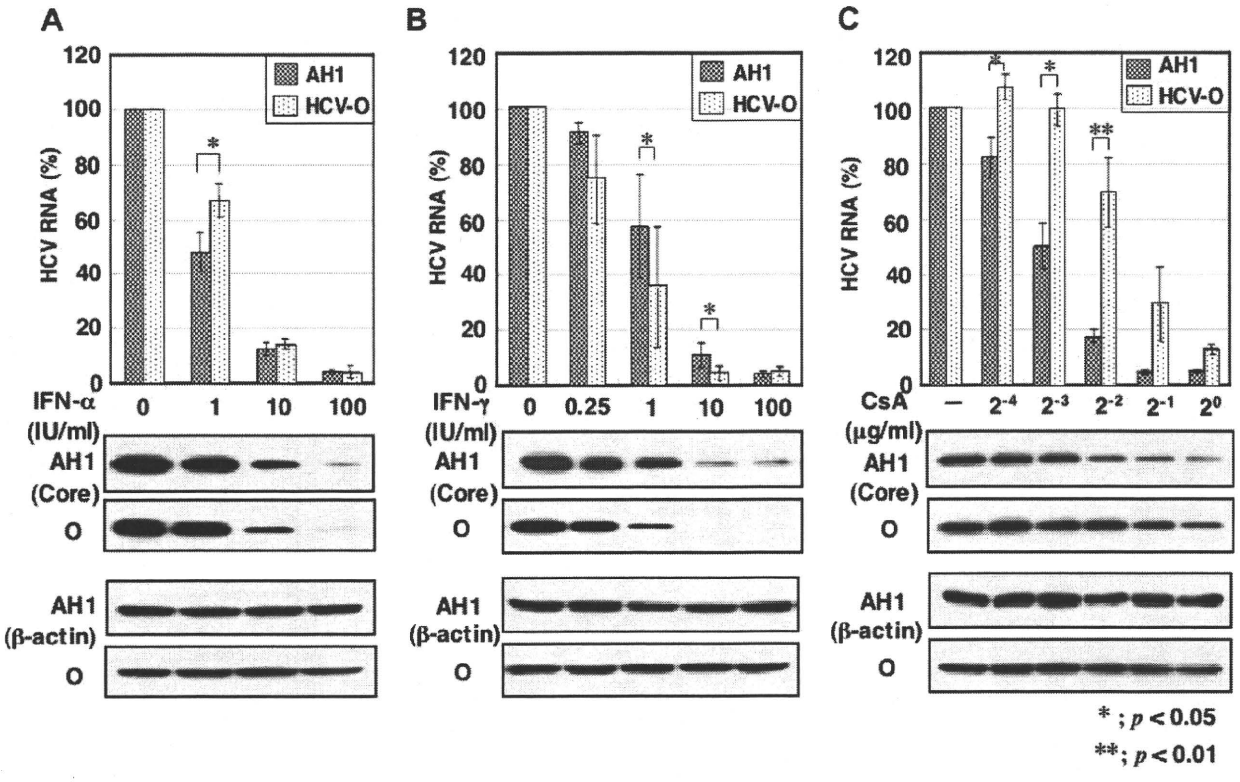

Fig. 3. The diverse effects of anti-HCV reagents on AH1 and HCV-O RNA replications. AH1 and O cells were treated with anti-HCV reagents for 72 h, and then extracted total RNAs and cell lysates were subjected to RT-qPCR for HCV 5′ UTR (each upper panel) and Western blot analysis for the core protein (each lower panel), respectively. (A) Effect of IFN-α. (B) Effect of IFN-γ. (C) Effect of CsA (Sigma).

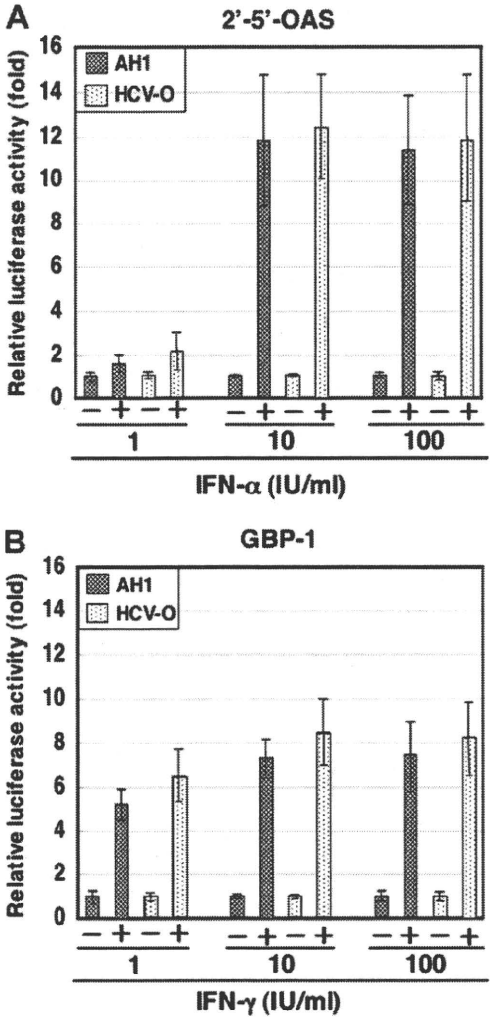

Fig. 4. Dual-luciferase reporter assay of IFN-α or IFN-γ-inducible gene promoter. AH1 and O cells were treated for 6 h with IFN-α or IFN-γ before the reporter assay. (A) 2′–5′-OAS gene promoter. (B) GBP-1 gene promoter.

with acute hepatitis C, and found diverse anti-HCV effects of IFN-γ and CsA between AH1 and HCV-O strains.

The levels of HCV replicon RNA and genome-length HCV RNA in sAH1 and AH1 cells were assigned to 3×10^7 and 2×10^7 copies/μg total RNA, respectively. These values are similar to those obtained from previously established HCV RNA replication systems [5]. Since known adaptive mutations (P1115L and V1897A) and additional conserved mutations (L1262S) were detected in the developed sAH1 replicon, these mutations may contribute to enhanced levels of RNA replication. The expression levels of genome-length HCV RNA and proteins observed in the present study suggest that genome-length HCV RNA replication efficiently occurs in AH1 cells, and that this RNA replication system is useful for comparison with already developed genome-length HCV RNA replication systems with HCV-N [7], Con-1 [8,9], or HCV-O [10] strains.

In the comparative analysis of genome-length HCV RNA replication systems with AH1 and HCV-O strains, we found that IFN-γ and CsA showed different anti-HCV profiles between AH1 and HCV-O strains. Regarding IFN-γ, RNA replication of the AH1 strain (EC_{50} = 1.9 IU/ml) was less sensitive than that of the HCV-O strain (EC_{50} = 0.3 IU/ml). Windisch et al. [18] have previously reported that RNA replication in an HCV replicon system using HuH-6 hepatoma cells is highly resistant (EC_{50} was more than 100 IU/ml) to IFN-γ, and that its resistant phenotype is not due to a general defect in the IFN-γ signaling pathway. In that study, they speculated that some mutations within a critical effector gene in HuH-6 cells might account for the inability of the cells to reduce the number of replicon RNAs in response to IFN-γ. Although such a possibility is not completely excluded, the diverse effects of IFN-γ observed in the present study were likely due to the difference in viral strains because RNA replication of the AH1 strain is still sensitive to IFN-γ. To clarify this point, development of an additional HCV RNA replication system such as an OR6 assay system with more quantitative reporter genes [10] is needed.

Regarding CsA, RNA replication of the AH1 strain (EC_{50} = 0.13 μg/ml) showed more sensitivity than that of the HCV-O strain (EC_{50} = 0.35 μg/ml). Ishii et al. [17] have previously reported that RNA replication of the JFH1 strain (genotype 2a) is less sensitive to CsA than genotype 1b strains, including the HCV-O strain. In that study, they concluded that the difference in sensitivity of JFH1 and genotype 1b strains to CsA could be attributed to characteristic differences in the HCV strains, not to the parent cell strain. In addition, sensitivity to CsA was almost the same among genotype 1b strains in that study. Therefore, we estimate that the AH1 strain is more sensitive to CsA than these genotype 1b strains examined to date. Further analysis will be necessary to clarify the mechanism underlying differences in sensitivity to CsA among genotype 1b strains.

In conclusion, an HCV RNA replication system with the AH1 strain would be useful for comparison with other strain-derived systems in various HCV studies, including analysis of the effects of anti-HCV reagents.

Acknowledgments

We thank T. Nakamura for technical assistance. We also thank A. Takamizawa and M. Kohara for the anti-NS3, NS4A, NS5A, and NS5B antibodies. This work was supported by grants-in-aid for a third-term comprehensive 10-year strategy for cancer control, and for research on hepatitis from the Ministry of Health, Labor, and Welfare of Japan.

Appendix A. Supplementary data

Supplementary data associated with this article can be found, in the online version, at doi:10.1016/j.bbrc.2008.04.005.

References

[1] D.L. Thomas, Hepatitis C epidemiology, Curr. Top. Microbiol. Immunol. 242 (2000) 25–41.
[2] N. Kato, M. Hijikata, Y. Ootsuyama, M. Nakagawa, S. Ohkoshi, T. Sugimurd, K. Sugimurd, Molecular cloning of the human hepatitis C virus genome from Japanese patients with non-A, non-B hepatitis, Proc. Natl. Acad. Sci. USA 87 (1990) 9524–9528.
[3] N. Kato, Molecular virology of hepatitis C virus, Acta Med. Okayama 55 (2001) 133–159.
[4] V. Lohmann, F. Korner, J. Koch, U. Herian, L. Theilmann, R. Bartenschlager, Replication of subgenomic hepatitis C virus RNAs in a hepatoma cell line, Science 285 (1999) 110–113.
[5] R. Bartenschlager, S. Sparacio, Hepatitis C virus molecular clones and their replication capacity in vivo and in cell culture, Virus Res. 127 (2007) 195–207.
[6] J.M. Pawlotsky, S. Chevaliez, J.G. McHutchison, The hepatitis C virus life cycle as a target for new antiviral therapies, Gastroenterology 132 (2007) 1979–1998.
[7] M. Ikeda, M. Yi, K. Li, S.M. Lemon, Selectable subgenomic and genome-length dicistronic RNAs derived from an infectious molecular clone of the HCV-N strain of hepatitis C virus replicate efficiently in cultured Huh7 cells, J. Virol. 76 (2002) 2997–3006.
[8] T. Pietschmann, V. Lohmann, A. Kaul, N. Krieger, G. Rinck, G. Rutter, D. Strand, R. Bartenschlager, Persistent and transient replication of full-length hepatitis C virus genomes in cell culture, J. Virol. 76 (2002) 4008–4021.
[9] K.J. Blight, J.A. McKeating, J. Marcotrigiano, C.M. Rice, Efficient replication of hepatitis C virus genotype 1a RNAs in cell culture, J. Virol. 77 (2003) 3181–3190.

[10] M. Ikeda, K. Abe, H. Dansako, T. Nakamura, K. Naka, N. Kato, Efficient replication of a full-length hepatitis C virus genome, strain O, in cell culture, and development of a luciferase reporter system, Biochem. Biophys. Res. Commun. 329 (2005) 1350–1359.
[11] N. Kato, K. Sugiyama, K. Namba, H. Dansako, T. Nakamura, M. Takami, K. Naka, A. Nozaki, K. Shimotohno, Establishment of a hepatitis C virus subgenomic replicon derived from human hepatocytes infected in vitro, Biochem. Biophys. Res. Commun. 306 (2003) 756–766.
[12] T. Wakita, T. Pietschmann, T. Kato, T. Date, M. Miyamoto, Z. Zhao, K. Murthy, A. Habermann, H.G. Krausslich, M. Mizokami, R. Bartenschlager, T.J. Liang, Production of infectious hepatitis C virus in tissue culture from a cloned viral genome, Nat. Med. 11 (2005) 791–796.
[13] N. Kato, H. Sekiya, Y. Ootsuyama, T. Nakazawa, M. Hijikata, S. Ohkoshi, K. Shimotohno, Humoral immune response to hypervariable region 1 of the putative envelope glycoprotein (gp70) of hepatitis C virus, J. Virol. 67 (1993) 3923–3930.
[14] H. Dansako, A. Naganuma, T. Nakamura, F. Ikeda, A. Nozaki, N. Kato, Differential activation of interferon-inducible genes by hepatitis C virus core protein mediated by the interferon stimulated response element, Virus Res. 97 (2003) 17–30.
[15] V. Lohmann, S. Hoffmann, U. Herian, F. Penin, R. Bartenschlager, Viral and cellular determinants of hepatitis C virus RNA replication in cell culture, J. Virol. 77 (2003) 3007–3019.
[16] K. Abe, M. Ikeda, H. Dansako, K. Naka, N. Kato, Cell culture-adaptive NS3 mutations required for the robust replication of genome-length hepatitis C virus RNA, Virus Res. 125 (2007) 88–97.
[17] N. Ishii, K. Watashi, T. Hishiki, K. Goto, D. Inoue, M. Hijikata, T. Wakita, N. Kato, K. Shimotohno, Diverse effects of cyclosporine on hepatitis C virus strain replication, J. Virol. 80 (2006) 4510–4520.
[18] MP. Windisch, M. Frese, A. Kaul, M. Trippler, V. Lohmann, R. Bartenschlager, Dissecting the interferon-induced inhibition of hepatitis C virus replication by using a novel host cell line, J. Virol. 79 (2005) 13778–13793.

Published online 4 November 2010

Nucleic Acids Research, 2011, Vol. 39, No. 2 e7
doi:10.1093/nar/gkq966

High-level expression by tissue/cancer-specific promoter with strict specificity using a single-adenoviral vector

Yumi Kanegae*, Miho Terashima, Saki Kondo, Hiromitsu Fukuda, Aya Maekawa, Zheng Pei and Izumu Saito

Laboratory of Molecular Genetics, Institute of Medical Science, University of Tokyo, 4-6-1 Shirokanedai, Minato-ku, Tokyo 108-8639, Japan

Received March 26, 2010; Revised September 24, 2010; Accepted October 3, 2010

Downloaded from nar.oxfordjournals.org at Ekigaku-Kyoshitsu (UNIV OF TOKYO) on February 23, 2011

ABSTRACT

Tissue-/cancer-specific promoters for use in adenovirus vectors (AdVs) are valuable for elucidating specific gene functions and for use in gene therapy. However, low activity, non-specific expression and size limitations in the vector are always problems. Here, we developed a 'double-unit' AdV containing the Cre gene under the control of an α-fetoprotein promoter near the right end of its genome and bearing a compact 'excisional-expression' unit consisting of a target cDNA 'upstream' of a potent promoter between two *lox*Ps near the left end of its genome. When Cre was expressed, the expression unit was excised as a circular molecule and strongly expressed. Undesired leak expression of Cre during virus preparation was completely suppressed by a dominant-negative Cre and a short-hairpin RNA against Cre. Using this novel construct, a very strict specificity was maintained while achieving a 40- to 90-fold higher expression level, compared with that attainable using a direct specific promoter. Therefore, the 'double-unit' AdV enabled us to produce a tissue-/cancer-specific promoter in an AdV with a high expression level and strict specificity.

INTRODUCTION

Because tissue-specific promoters enable us to express a gene in a cell-type-specific manner *in vivo* or in a primary tissue culture, such promoters offer an attractive approach to studying the specific functions of a gene product in the tissues of experimental animals, such as in the brain where cells of different types are present together in the same region. The use of transgenic/knockout mice and adenovirus vectors (AdVs) are the most common approaches for utilizing these promoters. Among such promoters, those specific to malignant cells may be valuable for specific gene therapy or the diagnosis of cancer.

However, one drawback of such promoters is that their expression levels are much lower than those of a versatile promoter, such as the cytomegalovirus (CMV) immediate-early, CAG (1) or EF1α (2) promoters. For example, the α-fetoprotein (AFP) promoter, which is a relatively strong promoter among tissue-specific promoters, is reported to be ~500-fold less active than the CAG promoter (3), limiting its usefulness. Another important problem associated with the use of these promoters is that their specificity was often not sufficiently strict. One possible reason is that the excised segment of a specific promoter lacks the sufficient control of specific silencers and shows some 'basal level' of expression. In some cases, the lack of specificity might arise from the DNA elements surrounding the promoter, rather than the intrinsic character of the specific promoter (4,5). In human gene therapy using AdV, a strict specificity is critically important for safety as well as efficacy.

As one solution, we previously reported a 'double-infection' method (3), in which the virtual activity of AFP promoter was increased by about 50-fold while maintaining a strict specificity. With this method, two AdVs are infected simultaneously: one AdV contains a 'switch unit' consisting of Cre gene under the control of AFP promoter, and the other AdV bears a 'target unit' consisting of the CAG promoter,

*To whom correspondence should be addressed. Tel: +81 3 54495556; Fax: +81 3 5449 5432; Email: kanegae@ims.u-tokyo.ac.jp
Present addresses:
Saki Kondo, Cell Regulation Laboratory, Paterson Institute for Cancer Research, University of Manchester, Wilmslow Road, Manchester, M20 4BX, UK
Hiromitsu Fukuda, Japan Animal Referral Medical Center, 2-5-8 Kuji, Takatsu-ku, Kawasaki-shi, Kanawawa 213-0032, Japan

© The Author(s) 2010. Published by Oxford University Press.
This is an Open Access article distributed under the terms of the Creative Commons Attribution Non-Commercial License (http://creativecommons.org/licenses/by-nc/2.5), which permits unrestricted non-commercial use, distribution, and reproduction in any medium, provided the original work is properly cited.

*lox*P, the stuffer sequence, second *lox*P, and a target cDNA, in that order. In non-hepatocarcinoma cells, the expression of the reporter cDNA remains turned off. However, in target hepatocarcinoma cells, AFP promoter in the switch unit of one AdV is turned on, leading to the production of Cre enzyme; this in turn leads to the excision of the stuffer sequence in the other AdV by Cre-mediated site-specific recombination, leaving the CAG promoter and the target gene connected only through a *lox*P sequence and enabling the strong expression of the target gene. Even when AFP promoter is weak and only a small quantity of Cre protein is produced, Cre can act as an enzyme multiple times, allowing most of the target AdV genomes to be processed eventually and accounting for the very high level of expression that can be obtained. The double infection method has been applied in numerous *in vivo* studies examining gene therapy for lung, colon and gastric cancers using the carcinoembryonic antigen promoter (6–10), for thyroid cancer using the thyroglobulin promoter (11), for hepatocellular carcinoma using AFP promoter (12), for prostate cancer using the prostate-specific antigen promoter (13) and for astrocytoma using the astrocytoma-specific promoter for GFAP (14). The method has also been applied in brain research using a modified, neuron-specific promoter of superior cervical ganglion 10 (15).

However, because the double-infection method uses two different AdVs simultaneously, controlling the infection is complicated and not often reproducible. Additionally, the toxicity and inflammation are at least doubled, compared with a single viral infection, for transducing the same amount of the target unit. Moreover, since a single cell infected with only one of the vectors does not produce any target protein, many such cells remain unused, causing a low expression as a result of dilution (12). Therefore, as a simpler, safer and more effective vector, an AdV bearing both the switch and the target unit simultaneously in a single genome is needed. However, the development of such an AdV has been regarded as being very difficult, since the sum of the lengths of both units exceeds the maximum length of the AdV genome. Furthermore, a leak in the expression of Cre can produce a large amount of stuffer-lacking AdV during vector preparation, causing severe non-specific expression. In addition, an enhancer of the potent promoter in the target unit may decrease the specificity of the specific promoter in the switch unit. Thus, a new vector is needed to solve these problems.

Here, we report the development and successful preparation of an AdV containing both units in a single genome. The vector, called a 'double-unit' AdV, possesses an extraordinary 'excisional-expression' structure and solves the aforementioned problems simultaneously, because the target unit of this vector lacks a stuffer sequence and because the target gene is expressed not from its genome, but from an excised circular DNA. The developed AdV shows a high level of expression (40- to 90-fold) while maintaining a very strict specificity.

MATERIALS AND METHODS

Cells and AdVs

The human embryo kidney cell line, 293 (16), constitutively expresses adenoviral E1 genes and supports the replication of E1-substituted AdV. HepG2 (17) and HuH7 (18) cells are human hepatocellular carcinoma cell lines that produce AFP. SK-Hep-1 (19) cells are a human hepatocellular carcinoma cell line that lack AFP production. HeLa cells, derived from cervical cancer, do not express AFP (20). The cell line CV1 is derived from African green monkey kidney. The AFP promoter used here was the (AB)2S6 AFP promoter (3). The EF1α promoter has been described previously (2). AxA2ANCre was described previously (3). AxLR14EL-AC, AxLR16EL-AC, AxLR16EFL, Ax-AC, AxNZ, AxLNZCAL, AxALNZCAL, AxA2AdsR and AxEFdsR are described for the first time in this work. AdVs described here were constructed using cosmid transfection (21). All the aforementioned viruses except for AxA2AdsR and AxEFdsR possessed E3 region with a 2.4-kb deletion, while the latter two viruses bore E3 region with the 1.9-kb deletion described in reference (21) (see 'Discussion' section). The switch unit was inserted at the *Sna*BI site (nt position 35 770), located 165-nt downstream from the right end of the adenovirus-5 (Ad5) genome. Because the standard Ad5 genome does not contain the *Sna*BI site, we generated a restriction site using nucleotide substitution, inserted a *Swa*I linker, and then cloned the switch unit. All the viruses were purified using a CsCl step gradient (22) and titrated using a method measuring 50% tissue culture infectious dose ($TCID_{50}$) (22); the viral particle: $TCID_{50}$ ratio was ~20:100, including double-unit viruses. The viral titer of all the AdV, including double-unit vectors was measured with $TCID_{50}$ using normal 293 cells.

Dominant negatives and shRNAs of Cre and isolation of Cre-suppressed 293 cells

dnCreRY was a dominant negative of Cre, where Arg173 and Tyr324 were mutated to Ala and Phe, respectively. pyCANCRYit2 is a plasmid expressing dnCreRY under the control of CAG promoter. The dnCreRY cDNA was excised as a *Sma*I-*Bgl*II fragment and inserted into pTrcHis2A (Invitrogen) between the *Ecl*36II and *Bgl*II sites under the *Escherichia coli* trc promoter (23). The *Bss*SI-*Sph*I fragment containing trc-dnCreRY was transferred upstream of the cos site of cosmid pAxLR16EL-AC and pAxLR14EL-AC, which were both derived from pAxcwit2 (21). The resulting cosmids were named ptdC-AxLR16EL-AC and ptdC-AxLR14EL-AC, respectively. shCreD (TA0493-4-D) was an shRNA of Cre, gatccGAAGCAACTCATCGATTGAtagtgctcctg gttgTCAATCGATGAGTTGCTTCtttttta (Cre sequences are in capitals), which efficiently suppressed Cre activity. TA0493-4-D was inserted under the human U6 promoter of plasmid pBAsi hU6 Pur (Takara Bio). The 293dnCreRY8 and 293shCreD13 were the best cell lines containing dnCreRY under the control of CAG promoter

Downloaded from nar.oxfordjournals.org at Ekigaku-Kyoshitsu (UNIV OF TOKYO) on February 23, 2011

and shCreD driven by human U6 promoter suppressing Cre activity among those tested, respectively.

To generate 293dnCreRY8, pBCANCRYSAPur was constructed, expressing dnCreRY under the control of the CAG promoter and the puromycin-resistant (Pur^R) gene under the control of the SV40 early promoter (Figure 5a). To generate 293shCreD13, pBSAPurhU6shCre was constructed, expressing one of the short-hairpin (sh) RNAs against Cre under the control of the human U6 promoter (Takara Bio) and the Pur^R gene identical to that expressed by pBCANCRYSAPur (Figure 5b). Ten micrograms of each plasmid DNA were transfected into 293 cells using Transfast^R (Promega). Two days after transfection, puromycin was added at a concentration of 2.5 μg/ml. We selected the cell line that most efficiently caused a reduction of Cre activity for the simultaneous transfection in Cre-expressing and target pCALNLG plasmids (24).

Preparation of total cell DNA for restriction-enzyme digestion and for real-time PCR

Infected cell DNA was prepared on a 24-well plate as previously described (25) with some modifications: the cells were suspended in 0.4 ml of TNE-PK [50 mM Tris–HCl (pH 8), 100mM NaCl, 10 mM EDTA, 100 mg/ml proteinase K], followed by the addition of SDS (final 0.1%). After incubation at 55°C for 2 h, the mixture was extracted once with phenol–chloroform and once with chloroform, and precipitated with 1 or 1.5 volumes of ethanol at −20°C for >1 h and then washed once with 70% ethanol. The pellet was dissolved with 50 ml of TE containing 20 mg/ml RNase A and stored at −20°C. This DNA was sufficient not only for real-time PCR but also for gel electrophoresis to observe the structure of the AdV genome.

To detect viral DNA, total DNA extracted from AxLR16EL-AC-infected, Cre-suppressed 293 cells in a 24-well plate was digested with *Bmg*BI. The *Bmg*BI recognition sequence, CACGTG, contains a -CG- dinucleotide, which is mostly methylated in the mammalian genome and cannot be cleaved by a restriction enzyme, while replicating adenoviral DNA is not methylated and can be cleaved. Consequently, restricted patterns of only adenoviral DNA can be seen.

Quantification of AdV transduction efficiency and expressed RNA

Total cell DNA was prepared as described above. Real-time PCR was performed to detect the adenovirus genome using a probe for the pIX gene, and human chromosome was simultaneously detected using a probe for the β-actin gene or the ornithine transcarbamylase (OTC) gene. The threshold cycle (cT) values were obtained. All the probes used in the study are shown in Table 1. The cT value of the AdV was corrected according to that for the human chromosome probe. The sequences of these probes were shown in Table 1. Infected cell RNA was prepared using the RNeasy protect mini kit (Qiagen) according to the manufacturer's protocol. To prepare the cDNA, the TaqMan Reverse Transcriptase Reagent kit (Applied BioSystems) was used. The sequences of the dsRed probes are shown in Table 1. The 18S rRNA primer used in the study were Ribosomal Eukaryotic 18S rRNA kit (Applied BioSystems).

Table 1. Sequences of probes used in real-time PCR

Probe[a]	Primer sequences[b]
AdV-1	F: TGTGATGGGCTCCAGCATT
	P: ATGGTCGCCCCGTCCTGCC
	R: TCGTAGGTCAAGGTAGTAGAGTTTGC
hOTC-1	F: CCACTACAAAATAAAGTGCAGCTGAA
	P: CCGTGACCTTCTCACTCTAAAAAACTT
	R: CTGATAGCCATAGCATATATTTAATTTCTTCTC
β-Act-1	F: CTCGCAGCTCACCATGGAT
	P: ATGATATCGCCGCGCTCGTCGT
	R: ATGCCGGAGCCGTTGTC
dsRed-1	F: GCAGCTGCCCGGCTACT
	P: CGTGGACTCCAAGCTGGACATCACCT
	R: CGATGGTGTAGTCCTCGTTGTG

18S rRNA primers used were Ribosomal Enkaryotic 18S rRNA kit (Applied BioSystems).
[a]Name of the probes. Reporters used were FAM except β-Act-1 (VIC reporter).
[b]F, forward primer; P, probe; R, reverse primer. Real-time PCR was purchased from Applied BioSystems.

To examine the expressed dsRed RNA, the cells were infected with AdV and total DNA and the total RNA was extracted. From the total DNA, the amounts of AdV genome and β-actin gene were simultaneously quantified using real-time PCR and the ratio of AdV genome per cell was obtained. Similarly, from the total RNA, the amounts of dsRed RNA and 18S-rRNA (the correction standard) were quantified using reverse transcription and real-time PCR, and the ratio of dsRed RNA to 18S-rRNA was obtained. Based on these results, the ratio of the dsRed RNA level between the two cell lines was calculated.

Detection of expressed fluorescence

To evaluate the different EF1α promoter versions, the cells were washed twice with Hank's balanced salt solution 3 days after transfection, and the intensity of GFP fluorescence was quantified using Fluoroskan Ascent FL (Labsystems) (26). Cells infected with AxLR16EL-AC and AxLR14EL-AC were sorted using dsRed fluorescence using FACS (FACSCalibur, Becton-Dikinson). The dsRed fluorescence was also measured using Ascent fluorescent meter. To calculate the relative strengths among the various promoters, the steady-state level of the expressed dsRed RNA together with the dsRed DNA in the AdV genome in infected cells was quantified using a real-time PCR (Prism 7000, Applied Biosystems), and the former value was divided by the latter.

RESULTS

Structure of 'double-unit' vector containing 'excisional-expression' unit

The structure of the 'double-unit' AdV vector AxLR16EL-AC is shown in Figure 1. This vector is a

Downloaded from nar.oxfordjournals.org at Ekigaku-Kyoshitsu (UNIV OF TOKYO) on February 23, 2011

first generation AdV containing the switch unit inserted near the right end of the adenovirus genome (27) (denoted in this paper at the E4 position) and the target unit inserted in the E1 region. Since the adenovirus genome can be packaged into a capsid up to ~105% of, or 2 kb more than, the wild-type genome size (28), it was impossible to generate an AdV containing both the switch and the target units using a typical construction strategy because of over-sizing. Therefore, to shorten the total length of the units, an 'excisional-expression' structure was adopted for the target unit. Although a typical target unit for conditional expression possesses (in order) the potent promoter, *lox*P, a stuffer sequence, a second *lox*P, cDNA and polyadenylation sequences (poly(A)), the excisional-expression unit lacks a stuffer sequence and instead consists of (in order) the right *lox*P, dsRed cDNA, poly(A), EF1α promoter and the left *lox*P (Figure 1, Target unit on AxLR16EL-AC). Notably, the dsRed cDNA is located not downstream, but 'upstream' of the EF1α promoter and, therefore, dsRed expression is turned off in the initial structure because AFP promoter does not function in non-hepatocarcinoma cells. However, once the AdV infects a hepatocarcinoma cell, AFP promoter is turned on and Cre enzyme is produced. Consequently, the expression unit of dsRed—EF1α promoter with one *lox*P is 'excised' as a circular molecule (Figure 1, middle), and the dsRed cDNA is now located downstream of the EF1α promoter, turning its expression on. At the same time, an AdV genome with one *lox*P is produced (Figure 1, lower, AxL-AC).

To minimize the genome size of the double-unit AdV: (i) a 0.55-kb section of the E3 region was deleted (see 'Discussion' section). In addition (ii) the EF1α promoter was shortened from an original length of 2.1 kb to lengths of 1.6 and 1.4 kb (named 16EF and 14EF, respectively). Unexpectedly, both the 16EF and 14EF promoters showed higher activity levels than the original EF1α promoter (Figure 2). As well; (iii) the 0.6-kb rabbit β-globin poly(A) sequence was truncated to 0.3 kb up to *Nde*I site. In addition to the size limitation, the double-unit AdV possesses several features that enable a very strict specificity (see Discussion section). As an improvement, the poly(A) sequence of 137 nt derived from the SV40 early region (*Hpa*I-*Bam*HI) was added in front of the dsRed cDNA plus the right *lox*P on the target unit (Figure 1, upper) based on the results of the following experiments. We constructed three AdVs containing the *lac*Z DNA tagged with the nuclear localization signal [NLacZ (3)] and their structures are shown in Figure 3a. CV1 cells were infected with each of these AdVs at multiplicity of infection (MOI) of 50 and, three days later, the *lac*Z expression of the infected cells was detected with X-gal staining. When cells were infected with AxNZ containing promoterless NLacZ (Figure 3a, top), weak but significant background expression was observed in most of the cells (Figure 3b, lower left); such expression was not observed in mock-infected cells (Figure 3b, upper left). When cells were infected with AxLNZCAL containing an excisional expression unit lacking the poly(A) in front of the NLacZ plus *lox*P (Figure 3a, middle), significant expression was observed (Figure 3b, upper right) and the expression level was much higher than that using AxNZ (lower left). We speculate from these results that a weak cryptic promoter may present upstream of the NLacZ and be activated by the enhancer of CAG promoter downstream of the NLacZ. Nevertheless, using AxALNLZCAL containing the excisional expression unit possessing poly(A) in front of NLacZ DNA plus *lox*P (Figure 3a, bottom), the background expression was almost disappeared (Figure 3b, lower right). The result showed that the inserted poly(A) sequence effectively reduced the background expression. The results were confirmed in the transfection experiments using the cosmids containing the full-length AdV genome (data not shown). Finally, we attempted to construct two AdVs, AxLR16EL-AC (104.9% of wild-type adenovirus genome) and AxLR14EL-AC (104.4%) containing the 16EF and 14EF promoters, respectively. The genome sizes of both AdVs were under the size limit.

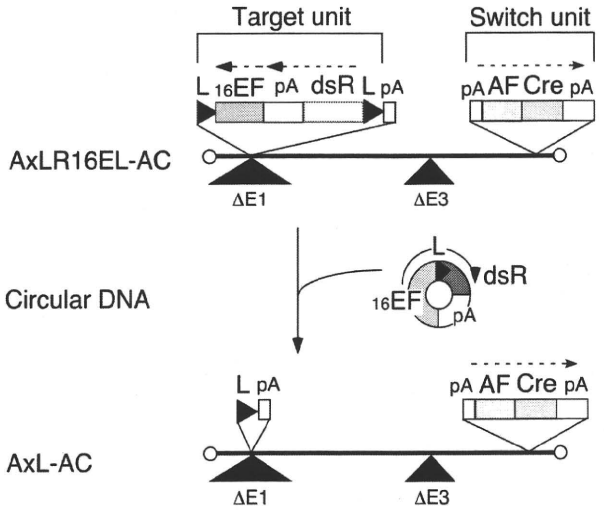

Figure 1. Structure of double-unit AdV and generation of expressing circular DNA. L, *lox*P; 16EF, shortened EF1α promoter; pA, poly(A) sequence; dsR, dsRed cDNA; AF, AFP promoter; Cre, nuclear localization signal-tagged Cre cDNA.

Leak expression of Cre both in *E. coli* and in 293 cells hampers the preparation of double-unit AdVs

Unexpectedly, during the construction of cosmids containing either AxLR16EL-AC or AxLR14EL-AC DNA (Figure 4a, dnCreRY –), we observed the co-generation of cosmids lacking the sequences between the two *lox*Ps (Figure 4b). The 2.5- and 2.7-kb bands (Figure 4c, lane 3) showed the presence of both cosmid DNA containing the AxL-AC genome and the excised circular DNA molecule, respectively. Judging from the intensities of the bands, the AxL-AC DNA accounted for ~15–20% of the midi-preparation (23) of *E. coli*. Thus, Cre must be expressed during cosmid preparation in *E. coli* DH5α despite the absence of an obvious *E. coli* promoter in the cosmid: the ampicillin promoter was present, but in the opposite orientation and ~20 kb away. Although the AxL-AC cosmid DNA was detected only faintly in the DNA of

Downloaded from nar.oxfordjournals.org at Ekigaku-Kyoshitsu (UNIV OF TOKYO) on February 23, 2011

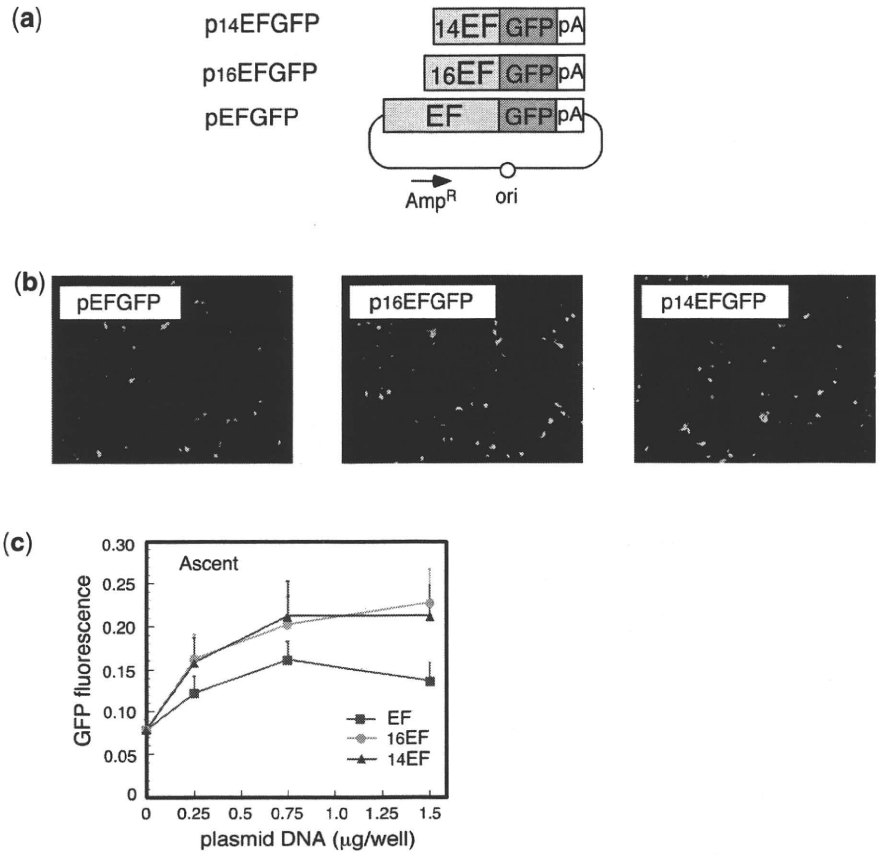

Figure 2. Expression of truncated EF1α promoter. (**a**) Structure of the plasmids expressing GFP under truncated EF1α promoter. The original EF1α promoter is 2.1-kb long. The 5′-end of 16EF was the *Ppu*MI site and that of 14EF was the *Blp*I site. (**b**) Images obtained using fluorescent microscopy. (**c**) Fluorescence measured using a fluoroscan plate reader. Vertical axis showed florescence in arbitrary unit; $n = 4$.

the mini-preparation (lane 2), it appeared to accumulate over time.

Furthermore, after the transfection of the cosmid DNA containing AxLR16EL-AC into 293 cells, all 12 of the viral clones that were generated were not the target virus, but apparently an AxL-AC virus. And three out of 18 viral clones derived from AxLR14EL-AC-containing cosmid DNA were mixtures of AxLR14EL-AC and AxL-AC viruses, while the other 15 clones were apparently pure AxL-AC virus (data not shown). These results showed that AFP promoter, which is thought to be inactive in non-hepatocellular 293 cells, certainly produced Cre in an amount sufficient to recombine the *lox*Ps on the AdV genome. This result probably occurred because even if the AFP promoter was strictly regulated, the AdV genome containing the switch unit of AFP promoter and Cre was amplified for 100 000 copies in one 293 cell and, consequently, an effective amount of Cre would be produced. Therefore, because of the leakage of Cre expression in both *E. coli* and 293 cells, double-unit vectors could not be prepared using conventional methods.

Successful suppression of leak expression of Cre using a dominant-negative of Cre and shRNA against Cre

To suppress the leak expression of Cre in *E. coli*, several dominant-negatives of Cre containing two amino acid mutations at the active center of Cre enzyme were constructed; dnCreRY, the dominant-negative that most efficiently suppressed Cre activity among those tested in co-transfection assays with a target plasmid, was then selected. Next, we constructed an expression unit producing dnCreRY under the control of the *trc* promoter of a *lac* operon system, and this unit was inserted into the cosmids containing AxLR16EL-AC and AxLR14EL-AC DNAs (Figure 4a, dnCreRY +). In the midi-preparation of this AxLR16EL-AC cosmid, neither the recombined AxL-AC-derived band nor the excised circular DNA molecule was detected with IPTG induction (Figure 4c, lane 7), showing that the production of dnCreRY successfully suppressed the leak expression of Cre in *E. coli*. Interestingly, since an apparent complete suppression was also observed without IPTG induction (lane 6), dnCreRY produced by the basal activity of the *trc* promoter was sufficient to suppress the leak expression of Cre effectively. Therefore, the problem of the leak expression of Cre in *E. coli* was solved.

To suppress the leak expression of Cre during AdV preparation in 293 cells, a plasmid expressing dnCreRY and a puromycin-resistant (PurR) gene (Figure 5a, upper) was transfected into 293 cells and the cell line 293dnCreRY8 was established; this cell line suppressed Cre activity the most efficiently. Virus clones were

Downloaded from nar.oxfordjournals.org at Ekigaku-Kyoshitsu (UNIV OF TOKYO) on February 23, 2011

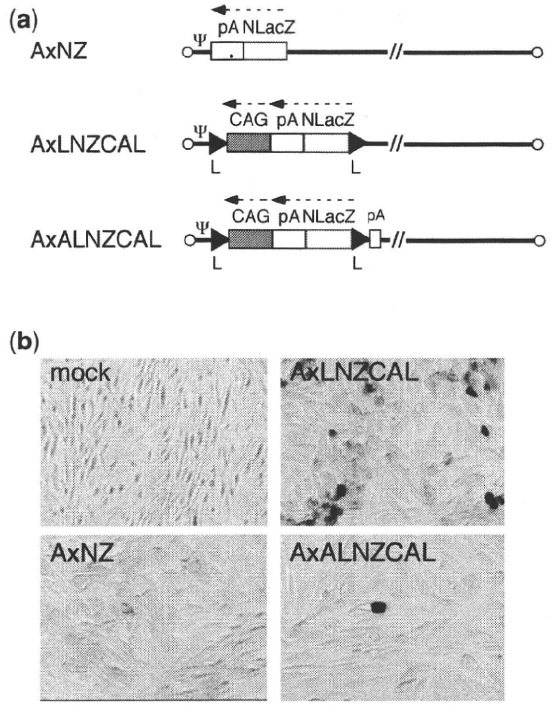

Figure 3. Suppression of the background expression by adding poly(A) sequence in front of *lacZ* DNA. (**a**) Structure of AdVs. (top) AxNZ contains the promoterless *lacZ* DNA; (middle) AxLNZCAL contains the excisional expression unit lacking poly(A) sequence in front of *lacZ* DNA plus right *lox*P; (bottom) AxALNZCAL contains that unit possessing poly(A) sequence in front of *lacZ* DNA plus right *lox*P. NlacZ, *lacZ* DNA tagged with NLS; Ψ, adenovirus packaging sequences; CAG, CAG promoter. The other representations are the same as in Figure 1. (**b**) Reduction of the 'background' expression observed using the promoterless *lacZ* DNA caused by addition of the poly(A) sequence. The infected CV1 cells were stained by X-gal. Very few dark-stained cells were observed in panels AxNZ (lower left) and AxALZCAL (lower right); the origin of these cells were unknown but possibly similar to those observed in Figure 7b and e.

obtained by transfecting linearized AxLR16EL-AC DNA, and the digestion of the viral genome with *Bmg*BI yielded a 1.8-kb band from an intact AxLR16EL-AC virus and a 1.4-kb band from a processed AxL-AC virus (Figure 5c). The 293dnCreRY8 cells did not produce pure AxLR16EL-AC virus, but instead produced mixtures of AxLR16EL-AC and AxL-AC (Figure 5a, lower, lanes 1, 3, 4 and 6) or mostly AxL-AC (lanes 2 and 5). Therefore, the suppression of Cre activity in the 293dnCreRY8 cells was not complete.

Meanwhile, several sh RNAs against Cre were constructed and screened, and shCreD was identified. Then, a plasmid expressing shCreD and PurR (Figure 5b, upper) was transfected into 293 cells, and the cell line 293shCreD13 was established. Unlike 293dnCreRY8, 293shCreD13 yielded mostly viral stocks of apparently pure AxLR16EL-AC virus (Figure 5b, lower, lanes 2, 3, 4 and 5), though some stocks were mixtures of both viruses (lanes 1 and 6). The AxLR16EL-AC virus in the apparently pure stocks was amplified in 293shCreD13 cells. To examine the 'leaky' expression level of Cre during the production of the double-unit vector in 293shCreD13 cells, an aliquot of AxLR16EL-AC viral stock was used to infect 293shCreD13 cells; then, to detect the viral genome, the total cell DNA was digested with *Bmg*BI. The 1.4-kb band produced by Cre recombination was not detected up to and including the third stock (data not shown) but, when the fourth stock purified using CsCl ultracentrifugation was examined, observed were the bands showing that the ratio of intact AxLR16EL-AC and 'leaked' AxL-AC was ~10:1 (Figure 5b, lower right). Of note, contamination with the AxL-AC virus does not cause any non-specific expression because Cre-processed AxL-AC virus does not contain an expression unit (Figure 1, bottom). An important point is that to prepare a double-unit AdV, the selection of an apparently

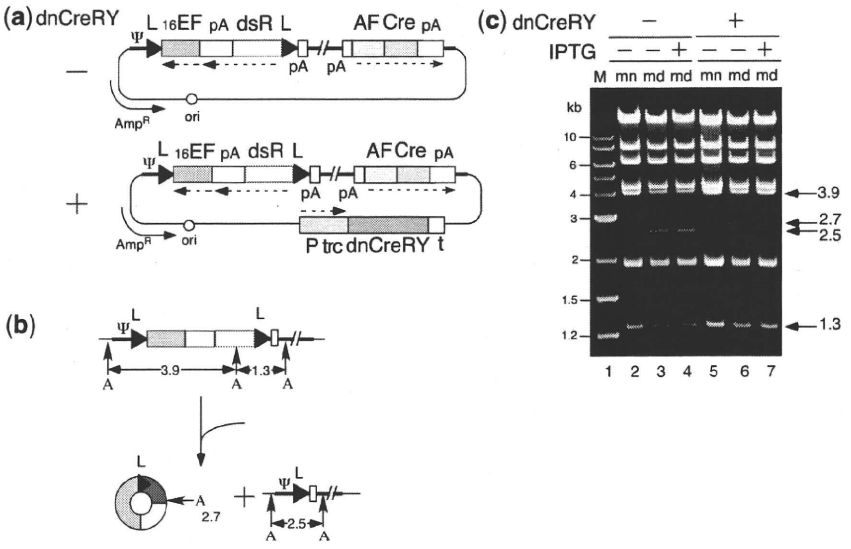

Figure 4. Leak expression of Cre in *E. coli*. Representations are the same as in Figure 1 unless otherwise stated. (**a**) Structure of cosmid generating double-unit AdV and expressing dnCreRY. Ψ, adenovirus packaging sequences; P trc, trc promoter; t, terminator. (**b**) Generation of Cre-processed molecules. A, *Ahd*I site. (**c**) Detection of Cre-processed molecules. M, 1-kb ladder marker; mn, mini-preparation; md; midi-preparation. The bands of 2.7 and 2.5 kb represent the generated circular DNA and Cre-processed DNA, respectively.

Downloaded from nar.oxfordjournals.org at Ekigaku-Kyoshitsu (UNIV OF TOKYO) on February 23, 2011

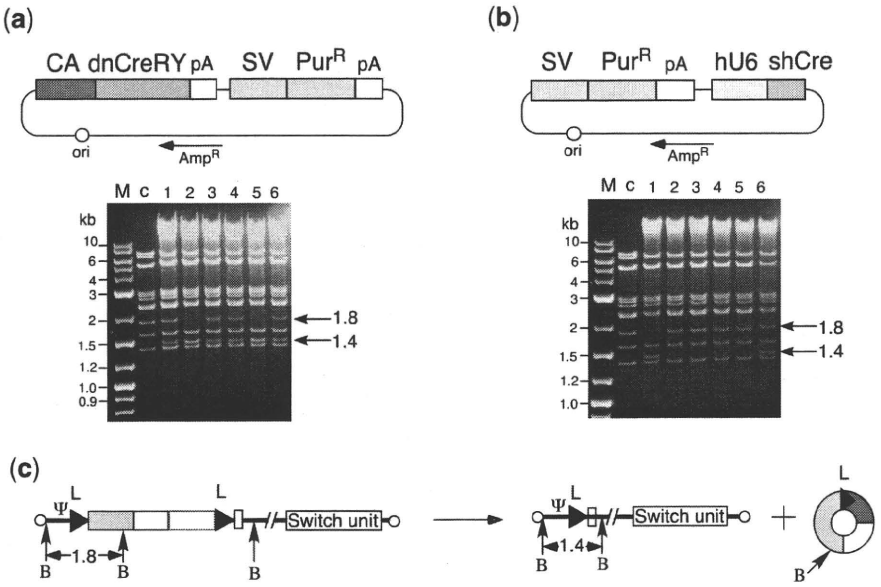

Figure 5. Establishment of 293 cell lines suppressing Cre activity. (**a**) Structure of plasmids expressing dnCreRY (upper) and DNA restriction pattern of double-unit viral clones produced in 293dnCreRY8 cells (lower). CA, CAG promoter; SV, SV40 early promoter; Pur^R, puromycin-resistant gene. The other representations are the same as in Figure 1. M, 1-kb ladder marker; c, restriction pattern of AxLR16EL-AC-containing cosmid DNA, presenting as a 1.8-kb band. (**b**) Structure of plasmids expressing shCre (upper) and DNA-restriction pattern of double-unit virus DNA of double-unit viral clones produced in 293shCreD13 cells (lower). hU6, human U6 promoter. P, purified/fourth stock was infected. The other representations are the same as in (a). (**c**) Generation of AxL-AC. B, *Bmg*BI site. The other representations are the same as in Figure 1. The presence or absence of circular 2.7-kb DNA was not clear in the gels of (a) and (b) because of the viral-derived bands of 2.9, 2.7 and 2.6 kb, but the circular DNA was hardly detected in the other experiment (data not shown). This result suggests that the production of the circular molecule occurs just after transfection and is consistent with the result that AxLR16EL-AC was stable up to the fourth stock.

Table 2. The viral titers of double-unit virus and the sprit viruses

Viruses[a]	Cells	Titers[b] ($TCID_{50}$)
AxLR16EL-AC	293shCreD13	1.1×10^{10}
AxLR16EL	Normal 293	4.7×10^{11}
Ax-AC	Normal 293	7.6×10^{10}

[a]The structure of AxLR16EL-AC is shown in Figure 1. The structures of split viruses, AxLR16EL and Ax-AC were shown in Figure 7a.
[b]Forth, purified viral stocks used in all experiments in this work.

pure first virus stock lacking AxL-AC as shown in Figure 5b, lower left, may be essential (see 'Discussion' section).

The 293shCreD13 cells grew well, similar to normal 293 cells, and the double-unit viruses were apparently able to proliferate in 293shCreD13 cells as well as normal E1-deficient AdV in 293 cells. Table 2 shows the titers of the double-unit virus AxLR16EL-AC produced in 293shCreD13 cells and of the split viruses shown in Figure 7a produced in normal 293 cells, all of which were used in this work. The titer of the double-unit virus was sufficiently high, though it was lower than those of the split viruses. One possible reason may be that the genome size of the former is near the upper limit. The AxLR14EL-AC virus was similarly prepared, and AxL-AC virus contamination was not detected in the third stock (data not shown).

The third viral stocks of double-unit virus without CsCl purification produced low but not negligible levels of non-specific dsRed expression when infected in HeLa cells (data not shown). Importantly, however, a viral preparation that was purified using a CsCl step gradient (22) did not produce any non-specific expression (see 'Discussion' section). Therefore, double-unit AdVs prepared in 293shCreD13 and purified using a CsCl step-gradient enabled the creation of viral stocks with a very strict specificity.

High-efficiency and very strict expression using double-unit AdV

The AxLR16EL-AC virus (at MOI of 5) was used to infect various cell types including HeLa (derived from non-liver carcinoma), SK-Hep1 (hepatocarcinoma-derived, non-producer of AFP), HuH-7 and HepG2 (hepatocarcinoma-derived producer of AFP). On day 3, high-level expressions of dsRed were observed in the infected HuH-7 and HepG2 cells (Figure 6h and k). Fluorescence-activated cell sorter (FACS) analyses showed that ~86 and 92% of these cells expressed detectable levels of dsRed, respectively (Figure 6i and l). In contrast, only one or two cells in a field of HeLa or SK-Hep1 cells expressed detectable levels of dsRed (Figure 6b and e), showing that the expression specificity of this vector was very strict. The FACS analyses confirmed that only 0.7 and 0.5% of the respective cells expressed detectable dsRed (Figure 6c and f). The results of dose-dependent experiments for all four cell lines confirmed the specificity of expression (Supplementary Figure S1).

Downloaded from nar.oxfordjournals.org at Ekigaku-Kyoshitsu (UNIV OF TOKYO) on February 23, 2011

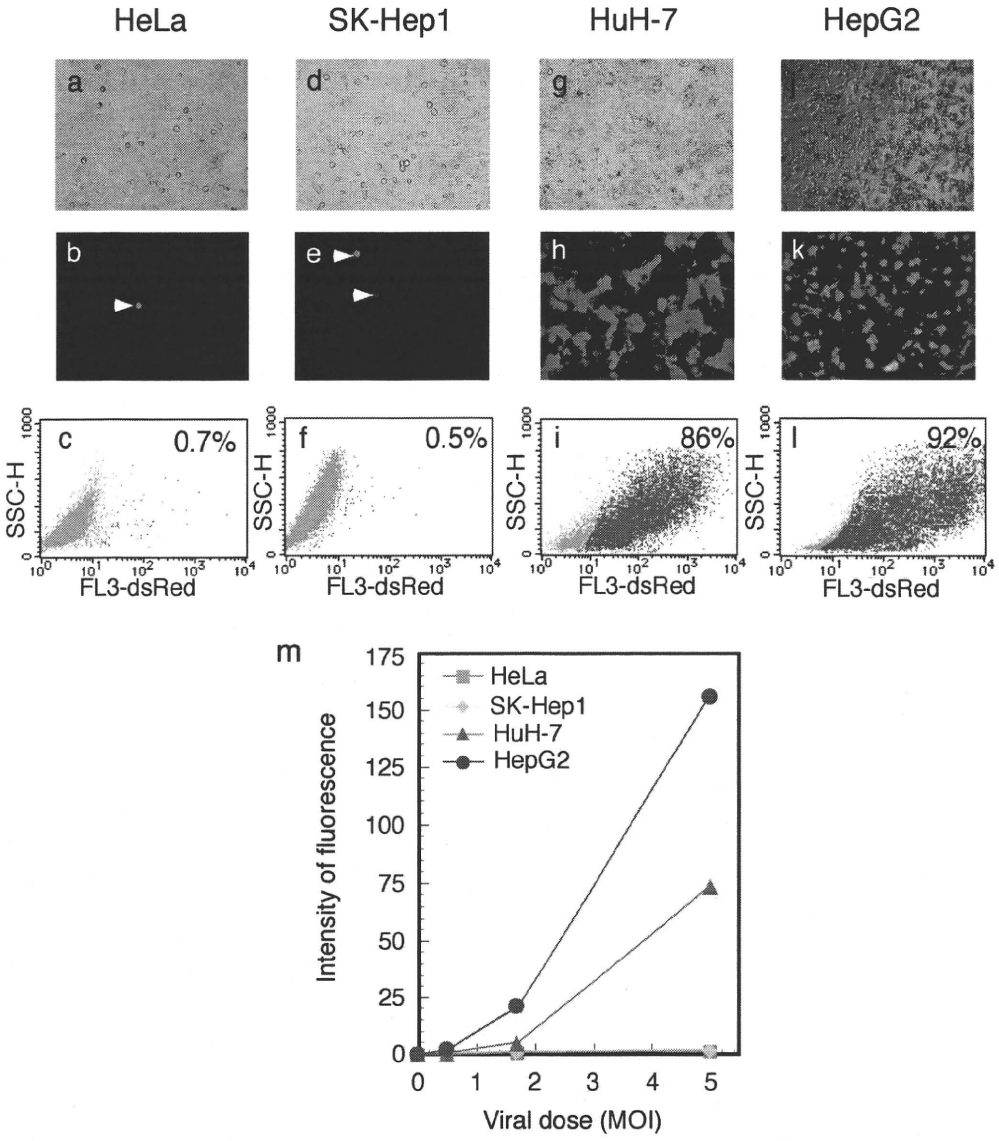

Figure 6. Specific and high-level expression of dsRed by AFP promoter using double-unit virus. Cells were infected with AxLR16EL-AC at MOI 5. (**a–c**) HeLa; (**d–f**) SK Hep-1; (**g–i**) HuH-7; (j, k and l) HepG2. (a, d, g and j) Phase-contrast microscopic views. (b, e, h and k) Images obtained using fluorescent microscopy. The arrow heads show exceptional cells with non-specific fluorescence. (c, f, i and l) FACS analysis of dsRed-expressing cells. SSC-H, side scattered light, high flow rate. (m) Dose responses of dsRed expression in the infected cells.

The dsRed expression was quantified using FACS by measuring the total sum of all cell fluorescence. The results showed that the ratio of the expressed mean fluorescence among the HeLa:SK-Hep1:HUH-7:HepG2 at MOI 5 in Figure 6c, f, i and l was 0.7:1:36.6:77.4, showing that the level of 'leaked' expression in the total cell population of AFP-negative cells compared with that in the AFP-positive cells was ~40 to 80 times less. The results of dose-dependent experiments are shown in Figure 6m. These results showed a very high expression and a strict specificity of this vector. Parallel to these FACS experiments, the transduction efficiency of the AdVs was measured by examining aliquots of all the four cell lines using real-time PCR as described in 'Materials and methods' section. The results indicated that the ratio of transduction efficiencies among HeLa, SK-Hep1, HuH-7 and HepG2 were 1.3:1:1.2:7.6, showing that the number of transduced AdV genomes present was almost the same for the first three cells. Therefore, these results confirmed very strict specificity of this vector for HeLa and SK-Hep1 cells. Meanwhile, HepG2 cells reproductively showed exceptionally high transduction efficiency. This seemed to be associated with the result that HepG2 showed much higher expression levels than HuH-7 cells (Figure 6m, at MOIs 1.7 and 5). Therefore, the very high expression level of HepG2 was partly explained by its exceptionally high transduction efficiency.

To examine the specificity of the double-unit vector, total RNA and DNA were extracted from AxLR16EL-AC-infected SK-Hep1 (AFP-negative) and HuH-7 (AFP-positive) cells. The amounts of expressed

Downloaded from nar.oxfordjournals.org at Ekigaku-Kyoshitsu (UNIV OF TOKYO) on February 23, 2011

dsRed RNAs and the transduced AdV genome were measured using real-time PCR as described in the Materials and methods section. The ratio of the dsRed RNA level corrected according to the transduced AdV genome between the two cell lines was calculated. The result showed that the dsRed RNA ratio of HuH-7 and SK-Hep1was 42.0:1, correlating well with the quantification of dsRed expression using FACS analyses. Identical experiments were performed using a control AdV AxCAdsRed expressing dsRed under the control of the CAG promoter instead of the double-unit vector. The result showed that the RNA ratio corrected according to the viral DNA amount between HuH-7 and SK-Hep1was 1.38:1, indicating that the activity of the CAG promoter was similar in both cell lines. These results indicated that the 'leak' level of the double-unit vector in the SK-Hep1 cells, compared with that in the HuH-7 cells, was ~1/40th of the expression level of HuH-7 cells (or 1/30th, based on of the CAG promoter control), demonstrating that the background level of double-unit vector in AFP-negative cells was again very low.

To examine the effect of combining the switch unit and the target unit into a single genome, we newly constructed two AdVs: AxLR16EL, containing only the target unit (Figure 7a, first), and Ax-AC, containing the switch unit at the E4 position (Figure 7a, second), as in AxLR16EL-AC. Then, the expression of the double-unit vector (AxLR16EL-AC) and the double infection of split viruses containing the excisional expression unit (AxLR16EL + Ax1AC) was examined using dsRed fluorescence. The double-unit vector showed a much higher fluorescence level than the double-infection method, as observed under a fluorescent microscope (Figure 7b). And the quantitative measurement of dsRed fluorescence showed that the former method produced 3.3-fold more dsRed protein than the latter method using an MOI of 13 (Figure 7c). The reason that the expression level was higher than that of the split viruses appears to be not only because the amount of the target virus was one half of the same total dose of the viruses, but also because in many cells, the split two vectors were not infected simultaneously or did not produce a sufficient amount of Cre during five days.

The steady-state levels of expressed dsRed RNA measured using real-time PCR in HuH-7 cells were compared with the direct expression under the control of AFP promoter (AxA2AdsR, Figure 7a), a double-unit vector (AxLR16EL-AC), a double-infection of split viruses (AxLR16EL + Ax-AC), and the expression under the control of EF1α promoter (AxEFdsR, Figure 7a) (Table 3). On Day 3, the double-unit vector expressed ~40-fold more dsRed RNA than the direct expression under the control of AFP promoter. Meanwhile, the double infection of split viruses (AxLR16EL + Ax-AC) expressed dsRed RNA at a level only 1/4th of that expressed by the double-unit vector, confirming the expression results (Figure 7c). Because the dsRed RNA expressed by the EF1α promoter (AxEFdsR) in HuH-7 cells was 480-fold higher than the direct expression of AFP promoter, the double-unit vector utilized ~1/10th of the EF1α promoter activity on day 3. However, on day 4, the

Table 3. Steady-state levels of expressed dsRed RNA in HuH-7 cells

AdV[a]	Ratio[b]
AxA2AdsR	1
AxLR16EL-AC	41
AxLR16EL + Ax-AC	10
AxEFdsR	480
AxLR16EL-AC (day 4)	91

Each experiment was performed twice to confirm the reproducibility; typical data are shown. The genome structures of the above viruses are shown in Figures 1 and 7a.

[a]HuH-7 cells were infected with each AdV at a MOI of 30. In the double infection, an MOI 15 of each virus was used.

[b]For each condition, the expressed dsRed RNA measured using real-time PCR was divided by the value obtained using the AxA2AdsR virus.

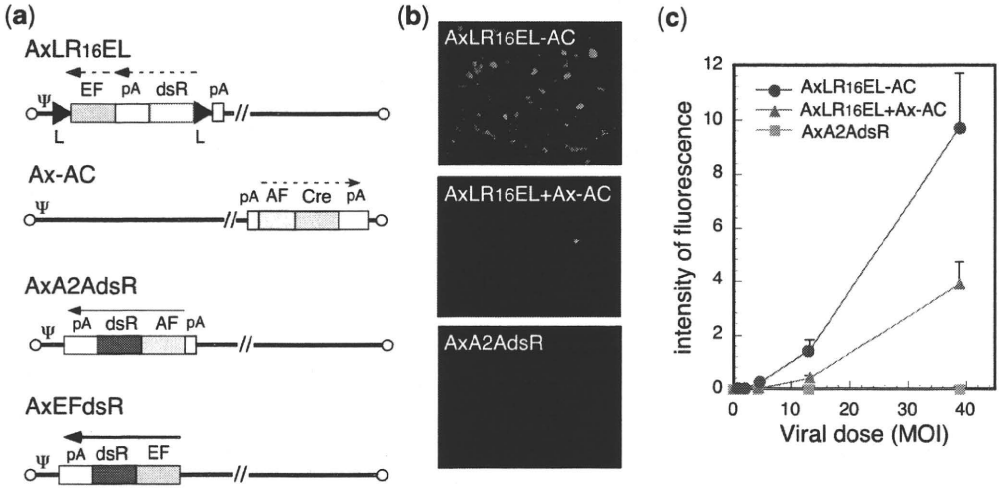

Figure 7. Simultaneous excisional expression in HuH-7 cells using double-infection method. (**a**) Structure of AdVs. The representations are the same as in Figure 1. (**b**) Images obtained using fluorescent microscopy. (**c**) Fluorescence measured using a fluoroscan plate reader.

Downloaded from nar.oxfordjournals.org at Ekigaku-Kyoshitsu (UNIV OF TOKYO) on February 23, 2011

expression of dsRed RNA reached ~90-fold when using the double-unit vector (Table 3); because such an increase in expression on later days was often observed in other double-unit experiments (data not shown), this result can likely be explained by the weak AFP promoter, since the very small amount of expressed Cre likely required a long time to process the target unit.

DISCUSSION

We developed a 'double-unit' AdV bearing an 'excisional-expression' structure and established a preparation method for this AdV. The AdV showed a high level of expression of the target gene under the control of a tissue/cancer-specific promoter, maintaining a very strict specificity. We observed that (i) because the vector was a first-generation AdV, it could be prepared on a large-scale without difficulty, and (ii) although a leak in Cre expression was observed during its preparation in *E. coli* and 293 cells, both problems were solved using a dominant-negative of Cre, dnCreRY, and an shRNA against Cre, shCreD, respectively. The complete suppression of Cre expression in 293 cells has been especially problematic, since AdV genome replication produces up to ~100 000 genome copies in each 293 cell. The key step in the production of the double-unit AdV was the selection of a clone lacking the AxL-AC virus (Figure 5b, lower left). Our results showed that severe AxL-AC generation caused by the leaky expression of Cre occurred 'before' the selection of a clone lacking the AxL-AC virus and that once such a clone was obtained, problematic deletion caused by 'leaked' Cre was not observed during the second to fourth production steps. Therefore, for the production of double-unit AdV even using 293shCreD13 cells, popular AdV-production protocols producing a pool of AdVs after transfection cannot be used.

As stated in the 'Introduction' section, this vector system is obviously superior to the 'double-infection' method (3); in the latter system, two viruses must be simultaneously transduced into a single cell for expression, and the infection of only one virus in a single cell is useless but causes similar viral toxic effects. Therefore, this new system will be particularly useful under diluted conditions, such as in animal experiments for basic research (unpublished data) as well as human gene therapy. Here, AFP promoter was used as one example, but obviously any tissue/cancer-specific promoter can be used. We intentionally did not adopt a CMV or CAG promoter, but instead used an EF1α promoter as a potent and non-specific promoter in the target unit because we have previously shown that the EF1α promoter hardly induces any inflammation as a result of AdV infection in an *in vivo* experiment, since no detectable induction of viral pIX production occurs (29). One report describing 'excisional expression' where a gene product was expressed only after excision by Cre from a Cre-excised circular molecule as described here has been previously published (30), but the purpose of this previous report was entirely different from that of the present work because the objective of the previous study was to examine persistent expression as a circular replicon using EB-viral oriP and used a double infection system using Cre-expressing AdV. Also, Yant *et al.* (31) reported another type of the 'excisional expression', where intron-containing transgenes were split and thus remained inactive until an FLP-mediated circularization restored the correct reading frame. The excision of an expression unit from the AdV genome by Cre or FLP has occasionally been reported (for examples, 32–34).

We observed a 'leak' in the expression level of the double-unit vector in an AFP-negative cell population amounting to ~1/40th of the expression level in HuH-7 cells measured using FACS as the total sum of all cell florescence, as stated in the Results section. While this level was very low, it was similar to the activity of the authentic AFP promoter in HuH-7 cells (Table 3). However, in AFP-negative cells infected with a double-unit virus, a small number of 'bright cells' highly expressing dsRed (Figure 6b, e and c, f) were present, increasing the apparent 'leaked' expression level.

Importantly, the specificity of the tissue/cancer promoter in this vector was very strictly maintained for a number of reasons. (i) Because the potent EF1α promoter in the target unit is present 'downstream' of the cDNA (Figure 1), an expression leak of the cDNA via this promoter is not possible until the promoter is translocated in front of the target cDNA by *lox*P recombination and circularization. (ii) The *lox*P-combined virus AxL-AC generated during the preparation of the double-unit virus does not contain an expression unit and hence does not cause non-specific expression. In contrast, the double-infection method always generates some stuffer-less, *lox*P-combined virus that causes non-specific expression because a small amount of such virus is generated even without Cre gene in AdV preparations, possibly through the homologous recombination of ~50 nt consisting of *lox*Ps and its surrounding sequences (3). (iii) Though conventional viral stock contains a small amount of circular DNA expressing the target gene and causing non-specific expression, it can be completely removed using a CsCl step gradient (22), since the DNA is much heavier than the virus particle. We previously observed that a DNA molecule in the viral stock can be 'transfected' into infected cells (35). (iv) The tissue-/cancer-specific promoter is inserted at the E4 position and is located farthest from the enhancer of a potent and non-specific EF1α promoter inserted at the E1-insertion site present near the left end of the genome. Therefore, the enhancer effect of the EF1α promoter on the specific AFP promoter is minimized. (v) A poly(A) sequence in front of the specific AFP promoter in the switch unit (Figure 1, upper right) suppresses non-specific transcription through a cryptic promoter present upstream of the specific promoter (3). And finally (vi) another poly(A) sequence in front of the *lox*P-cDNA in the target unit (Figure 1, upper left, and Figure 3) efficiently reduce the non-specific expression of cDNA probably caused by upstream cryptic promoters. We cannot argue whether the double-unit system is better in selectivity and less 'leaky' than the

Downloaded from nar.oxfordjournals.org at Ekigaku-Kyoshitsu (UNIV OF TOKYO) on February 23, 2011

authentic AFP promoter used here; for such conclusion further studies are needed using a more sensitive reporter system. However, because of these reasons above, the double-unit vector copes with high-level expression and strict specificity.

The total length of the AdV genome used in this method should not be more than ~38 kb (28). This means that the maximum length of a specific promoter plus target cDNA in this vector system with *Bsu*36I-*Blp*I E3 deletion (see below) should be 3.9 kb when the 14EF1α promoter is used and 4.5 kb when the 0.8-kb CMV promoter is used. This limitation of the length does not cause a problem in most cases. For example, because the AFP promoter used here is 2.2 kb in length, herpes thymidine-kinase cDNA (1.2 kb) or luciferase cDNA (1.7 kb) can be inserted; in fact, we constructed a double-unit AdV containing both AFP promoter and the thymidine-kinase gene, and animal experiments examining suicide-gene therapy are presently underway.

The problem of the genome length limitation can be solved using an AdV with a larger deletion in the E3 and E4 region. In the present study, AxLR14EL-AC and AxLR16EL-AC carried a *Bsu*36I-*Blp*I E3 deletion of 2433 bp, corresponding to 28 342–30 775-nt positions in the adenovirus type 5 map. The E3 region was 555-bp shorter than the *Xba*I-*Xba*I deleted E3 (21,27) and 252-bp longer than the *Bgl*II-*Bgl*II deleted E3 (36,37). We avoided using the *Bgl*II-*Bgl*II deleted E3 because L4 mRNAs of this AdV miss the L4 poly(A) sequences but use E3 poly(A) sequences, while *Xba*I-*Xba*I and *Bsu*36I-*Bpl*I deleted E3 both use the authentic L4 poly(A) sequences. Since an even shorter E3 region (27 865–30 995 nt) (36,38) and an E4 deletion (32 825–35 640 nt) (38) have been reported, the 3.9-kb limitation of the total lengths of a specific promoter plus cDNA when using AxLR14EL-AC could be enlarged up to 7.4 kb, if these vector constructs could be used.

Interestingly, Huyn *et al.* (39) recently reported an apparently related but different AdV system where, as the switch unit, a cancer-specific promoter produces a Gal4-VP16 fusion protein and, as the target unit, a Gal4-binding domain plus a CMV minimal promoter is used. They claimed that their method might be useful for visualizing cancer metastasis. A comparison of our vector with theirs would be difficult because they confirmed promoter specificity only in transfection experiments and because a cancer-specific promoter different from ours was used. Since our vector was developed with the goals of not only achieving a high expression level, but also of achieving a very low background in applications and ensuring the safety of gene therapy, the purposes of these studies are clearly different.

The method described here was totally different from that used for cancer-specific, replication-competent AdVs (for reviews, see references 40,41) in the field of cancer gene therapy. Although these AdVs use cancer-specific promoters, the adenoviruses replicate in the target cells and produce damaging effects through adenovirus gene expression in the target and surrounding cells. Although it has been reported that replication of E1-dereted AdV can be detected by Southern hybridization technique in HeLa cells at a higher MOI (42) and in other certain cells two weeks after infection (43), the replication level seemed too low to influence on the results described here.

The AdV system described here is probably useful for studying the function of a gene product in a specific tissue or organ. In any given tissue, several different sorts of cells are present: for example, neurons, glia cells and vascular endothelial cells are simultaneously present in neural tissue. Thus, this vector would be useful for expressing a gene selectively and efficiently in only one type of cell using a cell-specific promoter. This activity could enable novel, specific and effective therapies to be eveloped in the field of cancer gene therapy, and this strategy is now being tested. Furthermore, the application of this vector could be extended to include those where a high expression level and a rigid specificity are necessary.

The vector described here will be useful for many researchers using tissue/cancer-specific promoters. Plasmids suppressing Cre activity, cosmid cassettes for the construction of double-unit AdV containing *trc*-dnCreRY, and the 293 cell lines 293dnCreRY8 and 293shCreD13 are available from Riken Bioresource Bank (http://www.brc.riken.go.jp/) or in collaboration basis.

SUPPLEMENTARY DATA

Supplementary data are available at NAR Online.

ACKNOWLEDGMENTS

The authors thank Ms E. Kondo for her excellent secretarial assistance.

FUNDING

This work was supported by the Grant in Aid for Scientific Research on Priority Areas from Ministry of Education, Culture, Sports, Science and Technology, Japan (to I.S.). Funding for open access charge: Institute of Medical Science, University of Tokyo.

Conflict of interest statement. None declared.

REFFERENCES

1. Niwa,H., Yamamura,K. and Miyazaki,J. (1991) Efficient selection for high-expression transfectants with a novel eukaryotic vector. *Gene*, **108**, 193–199.
2. Kim,D.W., Uetsuki,T., Kaziro,Y., Yamaguchi,N. and Sugano,S. (1990) Use of the human elongation factor 1 alpha promoter as a versatile and efficient expression system. *Gene*, **91**, 217–223.
3. Sato,Y., Tanaka,K., Lee,G., Kanegae,Y., Sakai,Y., Kaneko,S., Nakabayashi,H., Tamaoki,T. and Saito,I. (1998) Enhanced and specific gene expression via tissue-specific production of Cre recombinase using adenovirus vector. *Biochem. Biophys. Res. Commun.*, **244**, 455–462.
4. Wilson,C., Bellen,H.J. and Gehring,W.J. (1990) Position effects on eukaryotic gene expression. *Annu. Rev. Cell Biol.*, **6**, 679–714.

Downloaded from nar.oxfordjournals.org at Ekigaku-Kyoshitsu (UNIV OF TOKYO) on February 23, 2011

5. Giraldo,P. and Montoliu,L. (2001) Size matters: use of YACs, BACs and PACs in transgenic animals. *Transgenic Res.*, **10**, 83–103.
6. Kijima,T., Osaki,T., Nishino,K., Kumagai,T., Funakoshi,T., Goto,H., Tachibana,I., Tanio,Y. and Kishimoto,T. (1999) Application of the Cre recombinase/*lox*P system further enhances antitumor effects in cell type-specific gene therapy against carcinoembryonic antigen-producing cancer. *Cancer Res.*, **59**, 4906–4911.
7. Ueda,K., Iwahashi,M., Nakamori,M., Nakamura,M., Yamaue,H. and Tanimura,H. (2000) Enhanced selective gene expression by adenovirus vector using Cre/*lox*P regulation system for human carcinoembryonic antigen-producing carcinoma. *Oncology*, **59**, 255–265.
8. Ueda,K., Iwahashi,M., Nakamori,M., Nakamura,M., Matsuura,I., Yamaue,H. and Tanimura,H. (2001) Carcinoembryonic antigen-specific suicide gene therapy of cytosine deaminase/5-fluorocytosine enhanced by the cre/*lox*P system in the orthotopic gastric carcinoma model. *Cancer Res.*, **61**, 6158–6162.
9. Goto,H., Osaki,T., Kijima,T., Nishino,K., Kumagai,T., Funakoshi,T., Kimura,H., Takeda,Y., Yoneda,T., Tachibana,I. *et al.* (2001) Gene therapy utilizing the Cre/*lox*P system selectively suppresses tumor growth of disseminated carcinoembryonic antigen-producing cancer cells. *Int. J. Cancer*, **94**, 414–419.
10. Ueda,K., Iwahashi,M., Nakamori,M., Nakamura,M., Matsuura,I., Ojima,T. and Yamaue,H. (2003) Improvement of carcinoembryonic antigen-specific prodrug gene therapy for experimental colon cancer. *Surgery*, **133**, 309–317.
11. Nagayama,Y., Nishihara,E., Iitaka,M., Namba,H., Yamashita,S. and Niwa,M. (1999) Enhanced efficacy of transcriptionally targeted suicide gene/prodrug therapy for thyroid carcinoma with the Cre-*lox*P system. *Cancer Res.*, **59**, 3049–3052.
12. Sakai,Y., Kaneko,S., Sato,Y., Kanegae,Y., Tamaoki,T., Saito,I. and Kobayashi,K. (2001) Gene therapy for hepatocellular carcinoma using two recombinant adenovirus vectors with alpha-fetoprotein promoter and Cre/*lox* P system. *J. Virol. Methods*, **92**, 5–17.
13. Yoshimura,I., Ikegami,S., Suzuki,S., Tadakuma,T. and Hayakawa,M. (2002) Adenovirus mediated prostate specific enzyme prodrug gene therapy using prostate specific antigen promoter enhanced by the Cre-*lox*P system. *J. Urol.*, **168**, 2659–2664.
14. Maeda,M., Namikawa,K., Kobayashi,I., Ohba,N., Takahara,Y., Kadono,C., Tanaka,A. and Kiyama,H. (2006) Targeted gene therapy toward astrocytoma using a Cre/*lox*P-based adenovirus system. *Brain Res.*, **1081**, 34–43.
15. Namikawa,K., Murakami,K., Okamoto,T., Okado,H. and Kiyama,H. (2006) Efficient generation of recombinant adenoviruses using adenovirus DNA-terminal protein complex and a cosmid bearing the full-length virus genome. *Gene Ther.*, **13**, 1244–1250.
16. Graham,F.L., Smiley,J., Russell,W.C. and Nairn,R. (1977) Characteristics of a human cell line transformed by DNA from human adenovirus type 5. *J. Gen. Virol.*, **36**, 59–74.
17. Aden,D.P., Fogel,A., Plotkin,S., Damjanov,I. and Knowles,B.B. (1979) Controlled synthesis of HBsAg in a differentiated human liver carcinoma-derived cell line. *Nature*, **282**, 615–616.
18. Nakabayashi,H., Taketa,K., Miyano,K., Yamane,T. and Sato,J. (1982) Growth of human hepatoma cells lines with differentiated functions in chemically defined medium. *Cancer Res.*, **42**, 3858–3863.
19. Fogh,J., Fogh,J.M. and Orfeo,T. (1977) One hundred and twenty-seven cultured human tumor cell lines producing tumors in nude mice. *J. Natl Cancer Inst.*, **59**, 221–226.
20. Ido,A., Nakata,K., Kato,Y., Nakao,K., Murata,K., Fujita,M., Ishii,N., Tamaoki,T., Shiku,H. and Nagataki,S. (1995) Gene therapy for hepatoma cells using a retrovirus vector carrying herpes simplex virus thymidine kinase gene under the control of human alpha-fetoprotein gene promoter. *Cancer Res.*, **55**, 3105–3109.
21. Fukuda,H., Terashima,M., Koshikawa,M., Kanegae,Y. and Saito,I. (2006) Possible mechanism of adenovirus generation from a cloned viral genome tagged with nucleotides at its ends. *Microbiol. Immunol.*, **50**, 643–654.
22. Kanegae,Y., Makimura,M. and Saito,I. (1994) A simple and efficient method for purification of infectious recombinant adenovirus. *Jpn. J. Med. Sci. Biol.*, **47**, 157–166.
23. Sambrook,J. and Russell. (1989) *Molecular Cloning: A Laboratory Manual*, Vol. 1, 3rd edn. Cold Spring Harbor Laboratory Press, Cold Spring Harbor, NY.
24. Kanegae,Y., Takamori,K., Sato,Y., Lee,G., Nakai,M. and Saito,I. (1996) Efficient gene activation system on mammalian cell chromosomes using recombinant adenovirus producing Cre recombinase. *Gene*, **181**, 207–212.
25. Saito,I., Oya,Y., Yamamoto,K., Yuasa,T. and Shimojo,H. (1985) Construction of nondefective adenovirus type 5 bearing a 2.8-kilobase hepatitis B virus DNA near the right end of its genome. *J. Virol.*, **54**, 711–719.
26. Kondo,S., Takata,Y., Nakano,M., Saito,I. and Kanegae,Y. (2009) Activities of various FLP recombinases expressed by adenovirus in mammalian cells. *J. Molec. Biol.*, **390**, 221–230.
27. Miyake,S., Makimura,M., Kanegae,Y., Harada,S., Sato,Y., Takamori,K., Tokuda,C. and Saito,I. (1996) Efficient generation of recombinant adenoviruses using adenovirus DNA-terminal protein complex and a cosmid bearing the full-length virus genome. *Proc. Natl Acad. Sci. USA*, **93**, 1320–1324.
28. Bett,A.J., Prevec,L. and Graham,F.L. (1993) Packaging capacity and stability of human adenovirus type 5 vectors. *J. Virol.*, **67**, 5911–5921.
29. Nakai,M., Komiya,K., Murata,M., Kimura,T., Kanaoka,M., Kanegae,Y. and Saito,I. (2007) Expression of pIX gene induced by transgene promoter: possible cause of host immune response in first-generation adenoviral vectors. *Hum. Gene Ther.*, **18**, 925–936.
30. Leblois,H., Roche,C., Di Falco,N., Orsini,C., Yeh,P. and Perricaudet,M. (2000) Stable transduction of actively dividing cells via a novel adenoviral/episomal vector. *Mol. Ther.*, **1**, 314–322.
31. Yant,S.R., Ehrhardt,A., Mikkelsen,J.G., Meuse,L., Pham,T. and Kay,M.A. (2002) Transposition from a gutless adeno-transposon vector stabilizes transgene expression in vivo. *Nat. Biotechnol.*, **20**, 999–1005.
32. Gil,J.S., Gallaher,S.D. and Berk,A.J. (2010) Delivery of an EBV episome by a self-circularizing helper-dependent adenovirus: long-term transgene expression in immunocompetent mice. *Gene Ther.*, doi:10.1038/gt.2010.75.
33. Dorigo,O., Gil,J.S., Gallaher,S.D., Tan,B.T., Castro,M.G., Lowenstein,P.R., Calos,M.P. and Berk,A.J. (2004) Development of a novel helper-dependent adenovirus-Epstein-Barr virus hybrid system for the stable transformation of mammalian cells. *J. Virol.*, **78**, 6556–6566.
34. Lee,J.H., Yi,S.M., Anderson,M.E., Berger,K.L., Welsh,M.J., Klingelhutz,A.J. and Ozbun,M.A. (2004) Propagation of infectious human papillomavirus type 16 by using an adenovirus and Cre/*Lox*P mechanism. *Proc. Natl Acad. Sci. USA*, **101**, 2094–2099.
35. Nakano,M., Odaka,K., Takahashi,Y., Ishimura,M., Saito,I. and Kanegae,Y. (2005) Production of viral vectors using recombinase-mediated cassette exchange. *Nucleic Acids Res.*, **33**, e76.
36. Bett,A.J., Haddara,W., Prevec,L. and Graham,F.L. (1994) An efficient and flexible system for construction of adenovirus vectors with insertions or deletions in early regions 1 and 3. *Proc. Natl Acad. Sci. USA*, **91**, 8802–8806.
37. Mizuguchi,H. and Kay,M.A. (1998) Efficient construction of a recombinant adenovirus vector by an improved in vitro ligation method. *Hum. Gene Ther.*, **9**, 2577–2583.
38. Mizuguchi,H. and Kay,M.A. (1999) A simple method for constructing E1- and E1/E4-deleted recombinant adenoviral vectors. *Hum. Gene Ther.*, **10**, 2013–2017.
39. Huyn,S.T., Burton,J.B., Sato,M., Carey,M., Gambhir,S.S. and Wu,L. (2009) A potent, imaging adenoviral vector driven by the cancer-selective mucin-1 promoter that targets breast cancer metastasis. *Clin. Cancer Res.*, **15**, 3126–3134.

Downloaded from nar.oxfordjournals.org at Ekigaku-Kyoshitsu (UNIV OF TOKYO) on February 23, 2011

40. Toth,K., Dhar,D. and Wold,W.S. (2010) Oncolytic (replication-competent) adenoviruses as anticancer agents. *Expert Opin. Biol. Ther.*, **10**, 353–368.
41. Mathis,J.M., Stoff-Khalili,M.A. and Curiel,D.T. (2005) Oncolytic adenoviruses – selective retargeting to tumor cells. *Oncogene*, **24**, 7775–7791.
42. Steinwaerder,D.S., Carlson,C.A. and Lieber,A. (2001) Human papilloma virus E6 and E7 proteins support DNA replication of adenoviruses deleted for the E1A and E1B genes. *Mol. Ther.*, **4**, 211–216.
43. Ghosh,S. and Duigou,G.J. (2005) Decreased replication ability of D1-deleted adenoviruses correlates with increased brain tumor malignancy. *Cancer Res.*, **65**, 8936–8943.

Downloaded from nar.oxfordjournals.org at Ekigaku-Kyoshitsu (UNIV OF TOKYO) on February 23, 2011

doi:10.1016/j.jmb.2009.04.057 J. Mol. Biol. (2009) 390, 221–230

JMB

Available online at www.sciencedirect.com

ScienceDirect

ELSEVIER

Activities of Various FLP Recombinases Expressed by Adenovirus Vectors in Mammalian Cells

Saki Kondo[1], Yuki Takata[1,3], Masakazu Nakano[1,2], Izumu Saito[1] and Yumi Kanegae[1]*

[1]*Laboratory of Molecular Genetics, Institute of Medical Science, University of Tokyo, 4-6-1 Shirokanedai, Minato-ku, Tokyo 108-8639, Japan*

[2]*Department of Genomic Medical Sciences, Kyoto Prefectural University of Medicine, Kawaramachi-Hirokoji Kamigyo-ku, Kyoto 602-8566, Japan*

[3]*Manufacturing Technology Kokando Co.,Ltd, 2-9-1 Umezawacho,Toyama 930-0055, Japan*

Received 19 December 2008; received in revised form 24 April 2009; accepted 27 April 2009
Available online 3 May 2009

FLP, like Cre, is a frequently employed site-specific recombinase. Because wild-type FLP (wtFLP) is thermolabile, a thermostable FLP mutant (FLPe) has been developed for efficient recombination of FLP in studies using mammalian cells and animals. FLPe and wtFLP have been compared in multiple assays *in vitro* and *in vivo*, and in mouse genetics, FLPe has been shown to be very effective like Cre. Here we show an adenovirus vector (AdV) system to be valuable for quantitative measurements of the enzyme activity in mammalian cells and, using this system, precisely compare activities of wtFLP and FLPe. Unexpectedly, we found that the recombination efficiency of FLPe enzyme was lower on a molar basis than that of wtFLP even at 37 °C and, consequently, that the higher recombination yield per transduced AdV genome expressing FLPe compared to wtFLP was due not to inherently higher enzyme activity, but rather to higher steady-state levels of FLPe by its thermostability. Therefore, trying to increase FLPe levels further, we generated a "humanized" FLPe (hFLPe) gene with codon usage optimized for mammals. hFLPe produced about 10-fold more FLPe enzyme in transfection experiments than FLPe, as expected. However, hFLPe-expressing AdV was unstable and could not be prepared without deletion, suggesting that a subtle deleterious effect of FLP on 293 cells may exist. With hFLPe-expressing AdV thus unavailable, of the AdV constructs tested, AdV-expressing FLPe yielded the most recombined targets, despite the lower recombination efficiency of FLPe per enzyme molecule compared with that of wtFLP. We found hFLPe to be valuable for plasmid transfection, and its properties are probably suitable for experiments involving cell lines and transgenic mice.

© 2009 Elsevier Ltd. All rights reserved.

Edited by B. Connolly

Keywords: FLP; FLPe; recombinase; adenovirus vector; mammalian cell

Introduction

Site-specific recombinases for analyzing gene function are an important tool for both *in vitro* and *in vivo* studies. Recombinases can induce a deletion, insertion, or inversion of DNA sequences by connecting their target sequences without requiring any other specific factor; these DNA rearrangements can mediate gene activation and inactivation. FLP recombinase, derived from *Saccharomyces cerevisiae*, is a member of the λ integrase family and recognizes a 34-base-pair (bp) FRT (FLP recognition site) recognition target sequence; by now well characterized, FLP has been utilized for gene regulation in plants,[1,2] *Drosophila*,[3,4] mammalian cell cultures,[5–7] and mouse transgenics.[8–10] Another site-specific recombinase, Cre[11–14] (derived from bacteriophage P1), is used similarly; however, Cre has been reported to be toxic to cells not only during constitutive expression,[15–17] but also during transient expression.[18] Therefore, the use of Cre is sometimes problematic. In contrast, FLP has never been reported to be toxic.

While Cre activity is stable at temperatures over 37 °C,[19] the optimum temperature of wild-type FLP (wtFLP) is about 30 °C due to its poor thermostability.[19] The drawback was overcome by the development of a thermostable mutant of FLP

*Corresponding author. E-mail address: kanegae@ims.u-tokyo.ac.jp.

Abbreviations used: wt, wild type; wtFLP, wild-type FLP; FLPe, thermostable FLP mutant; AdV, adenovirus vector; hFLPe, humanized FLPe; FRT, FLP recognition site; ES, embryonic stem; GFP, green fluorescent protein; pA, polyadenylation; FACS, fluorescence-activated cell sorter; MOI, multiplicity of infection.

0022-2836/$ - see front matter © 2009 Elsevier Ltd. All rights reserved.